USED FUEL DISPOSITION CAMPAIGN

Radiolysis Model Sensitivity Analysis for a Used Fuel Storage Canister

Fuel Cycle Research & Development

Prepared for
U.S. Department of Energy
Used Fuel Disposition
Campaign

Rick Wittman

September 20, 2013

FCRD-UFD-2013-000357

PNNL-22773

Submitted by:

Signature on file

Brady D. Hanson
Lab Lead ST Experiments

EXECUTIVE SUMMARY

This report fulfills the M3 milestone (M3FT-13PN0810027) to report on a radiolysis computer model analysis that estimates the generation of radiolytic products for a storage canister. The analysis considers radiolysis outside storage canister walls and within the canister fill gas over a possible 300-year lifetime. Previous work relied on estimates based directly on a water radiolysis G-value.[a] This work also includes that effect with the addition of coupled kinetics for 111 reactions for 40 gas species to account for radiolytic-induced chemistry, which includes water recombination and reactions with air.

The main results for radiolysis inside the canister fill gas are described as follows.

- Significant radiolysis of water vapor requires the presence of residual air to disable recombination.
- Reactions between residual water (1 L) and air in 4500 L of free space result in percent levels of H_2, O_2 and HNO_3 at 300 years, and about one-half the maximum values reached in the first 16 years.
- Calculations indicate that a much greater volume of residual water (20 L) would be required to reach the 4% H_2 flammability limit in 16 years, and between 3 and 4 L of water would be required to reach the 4% H_2 flammability limit in 300 years.
- Increased residual air results in greater H_2 and HNO_3 concentrations, but also in the depletion of O_2 because it is more effectively removed by a radiolytically induced reaction with N_2.
- For lower (0.1%) residual air, O_2 is initially depleted and then generated for storage times greater than 50 years, resulting in approximately 0.5% O_2.
- For lower (0.1 L) residual water and 1% air, all radiolytic products are less than 1%.

The main results for radiolysis outside the canister follow.

- The main radiolytic products formed in moist air are HNO_3, N_2O, NO_2, CO, and small amounts of O_3.
- Even for extremely long residence times, the highest concentrations are less than 50 ppm and are less than 1 ppm for more typical flow conditions.
- Dry air gives similar concentrations as moist air with the exception of increased NO_2 and the near absence of HNO_3.

[a] Reed DT. 1991. *Progress in Assessing the Effect of Ionizing Radiation on the Anticipated Waste Package Environment at the Yucca MountainPotential Repository Site*, ANL/CP—72981; CONF-910945-6. Paper for Focus '91, Nuclear Waste Packaging Sponsered by The American Nuclear Society and The American Society of Materials, Las Vegas, Nevada, September 29-October 2, 1991. Available at http://www.osti.gov/scitech/biblio/138264.

In both cases, it was determined that H_2O_2 formation in the gas was insignificant (<10 ppm), but could be significant (10-200 μM) for radiolysis of a thin layer of residual liquid water on surfaces. Additionally, a significant level of dissolved O_2 would be required for H_2O_2 to reach 100 μM in the liquid water inside a canister.

ACKNOWLEDGMENTS

We thank Edgar Buck and Chuck Soderquist for helpful discussions on radiolysis chemistry and its effects on nuclear materials. We thank Edgar Buck, Carlos Jové-Colón, and David Sassani for supporting and helping in the development of an aqueous phase radiolysis model for the used fuel disposition fuel degradation studies that helped make this work possible.

CONTENTS

FIGURES

TABLES

ACRONYMS

ASTM	ASTM International
DOE	U.S. Department of Energy
DOE-NE	U.S. Department of Energy Office of Nuclear Energy
GWd	gigawatt-day
MTU	metric tons (Tonnes) of uranium
ODE	ordinary differential equation
PNNL	Pacific Northwest National Laboratory
RH	relative humidity
SNF	spent nuclear fuel
UFDC	Used Fuel Disposition Campaign
UNF	used nuclear fuel

USED FUEL DISPOSITION CAMPAIGN
Radiolysis Model Sensitivity Analysis for a Used Fuel Storage Canister

1. INTRODUCTION

The U.S. Department of Energy Office of Nuclear Energy (DOE-NE), Office of Fuel Cycle Technology has established the Used Fuel Disposition Campaign (UFDC) to conduct the research and development activities related to storage, transportation, and disposal of used nuclear fuel (UNF) and high-level radioactive waste. Within the UFDC, the storage and transportation task has been created to address issues of extended or long-term storage and transportation. The near-term objectives of the storage and transportation task are to use a science-based, engineering-driven approach to develop the technical bases

- to support the continued safe and secure storage of UNF for extended periods
- for retrieval of UNF after extended storage
- for transport of high burnup fuel, as well as low and high burnup fuel after dry storage.

This report is in response to a cross-cutting gap analysis recommendation to address the potential for internal and external canister corrosion and hydrogen buildup (Hanson et al. 2012a, 2012b).

Concerns of radiolysis of water and water vapor remaining in cask, which could result in corrosion (especially of cladding) or result in the generation of hydrogen that could result in flammability concerns has led some regulators, such as in France, to require monitoring of packages for hydrogen. In addition, concerns of radiolysis of water and water vapor exterior to a canister, as air flows through the overpack, have previously been raised.

To address the above recommendation and concerns, this report documents the development of a radiolysis model to predict the radiolytically induced generation of hydrogen and corrosive products such as H_2O_2, O_2, NO_2, NO, and HNO_3 within and around a canister. Section 2 contains a description of the radiolysis model and a comparison with literature results as a modest step toward model verification. Section 3 reports on the radiolysis model analysis of various canister conditions to estimate the variability and possible bounds on radiolysis product concentrations. Section 4 summarizes the results of the study. The Appendixes provide the radiolysis model input files and FORTRAN listing of the computer program.

2. MODEL DESCRIPTION

The radiolysis model developed for this analysis is formulated as a set of coupled kinetics equations for the reactions of gaseous species assumed to exist in the open environment outside of the canister and inside the canister fill gas. Radiolytic species are generated at a rate that is determined by the dose rate induced by the radiation field and the concentrations of air and water vapor present. Subsequent reactions of the radiolytic species are then computed, based on the reaction kinetics. The model inputs are the reaction rate constants, the temperature and dose rate, the radiolytic G-values, and the initial concentrations. The current model approximates the bulk composition of the gas as a uniform system without accounting for localized hot spots with possible diffusive and convective flow. The open gas surrounding the canister is assumed to have a residence time based on varying the volumetric flow around the canister.

2.1 Model Definition

The coupled kinetics rate equations for the gas species concentrations $[A_i]$ are

$$\frac{d\,[A_i]}{dt} + \frac{R}{V}\left([A_i] - [A_i]_0\right) = \dot{d}\sum_{g=1}^{N_g} G_i^{(g)} w_g\,[A_g] + \sum_{r=1}^{N_r} k_{ir} \prod_{j_r=1}^{n_r} [A_{j_r}]^{O_{j_r}} \tag{1}$$

with rate constants k_{ir}, dose rate $\dot{d}$, molecular weights w_g and radiolytic generation constants G_i. The resident time for external air around the canister is V/R, where V is the effective air volume and R is the volume flow rate of external air with composition $[A_i]_0$ that enters the region. For brevity, the "sum-of-products" on right-hand side of Eq. 1 expresses the sum of the product of reactant concentrations entering with reaction order O_{jr} where the multiplication-index j_r is over the n_r reactants for reaction index r. The notation includes the final state order of component i produced by writing the rate constants k_{ir}, dependent on index i, but of course that dependence only amounts to an integer (which could be zero) multiplied by the reaction rate constants. The radiolysis model consists of 111 reactions for water vapor and air (N_2, O_2, CO_2). The temperature dependence of the rate constants is given according to

$$k_{ir} = k_{ir}^{(0)}\, T^{x_r} \exp\left(-E_r/T\right) \tag{2}$$

where T is in Kelvin and the constants $k^{(0)}$, x_r and E_r for all reactions are given in Appendix A.

The G-values account for the effective fraction of radiative energy that contributes to the formation of the dominant radiolytic species. Together with ionization, the interaction of energetic radiation with air can generate very short-lived (10^{-15} s) electronic excitations that favorably de-excite through intermediate atomic and molecular radicals. The reaction of these radicals with the surrounding environment occurs on the scale of 10^{-9} s resulting in several dominant species—both stable and unstable. We take the conventional approach in representing the radiolytically generated species at the later time scale with effective G-values. Values for gamma radiolysis used in this work are given in Table 2-1.

Table 2-1. G-values for Air (Bulearcă et al. 2010)

	G (particles/100-eV)			
Species	H_2O	N_2	O_2	CO_2
H_2O	-7.350	0.000	0.000	0.000
$\cdot H$	7.400	0.000	0.000	0.000
$\cdot OH$	6.300	0.000	0.000	0.000
H_2	0.500	0.000	0.000	0.000
O_2	0.000	0.000	-5.300	0.000
$\cdot O$	1.050	0.000	5.230	5.020
O_2^+	0.000	0.000	2.070	0.000
O^+	0.000	0.000	1.230	0.210
e^-	0.000	2.960	3.300	2.960
N_2	0.000	-4.140	0.000	0.000
$\cdot N$	0.000	0.295	0.000	0.000
$N(^2D)$	0.000	0.885	0.000	0.000
$N(^4S)$	0.000	1.870	0.000	0.000
N_2^+	0.000	2.270	0.000	0.000
N^+	0.000	0.690	0.000	0.000
CO_2	0.000	0.000	0.000	-7.470
CO	0.000	0.000	0.000	4.720
CO^+	0.000	0.000	0.000	0.510
CO_2^+	0.000	0.000	0.000	2.240

The reactions, the G-values, and the species considered are the ones typically modeled for atmospheric chemistry (Atkinson et al. 2004) and gas treatment applications (Bulearcă et al. 2010), as well as for steam radiolysis occurring in nuclear power plant operations (Arkhipov et al. 2007). Of course, many other reactions could be considered—the motivation here is to consider a sufficient set to account for H_2 generation and the generation of corrosive products (e.g., HNO_3, O_2, H_2O_2) affecting the integrity of the used fuel storage canisters. Initially, 101 reactions from references (Arkhipov et al. 2007, Atkinson et al. 2004, Bulearcă et al. 2010) were considered. The last 10 reactions (102-111) were added for the physical consistency of ensuring the concentrations of charged and unstable species go to zero as the dose rate goes to zero under any conditions. Sets of reactions in the literature tend to satisfy that condition for a specific application, but not always for general conditions occurring for a sensitivity analysis. For this work, the 40 species of Table 2-2 are considered.

We set up the kinetics equations (Eq. 1) in FORTRAN and used the subroutine DLSODA from the set of ordinary differential equation (ODE) solvers of reference (Hindmarsh 1983, Brown and Hindmarsh 1989) to solve for the concentrations over about 200,000 logarithmic time steps out to 300 years. Both charge balance and atom balance are implicit in the reactions and for the G-values—additionally, they are used to confirm numerical consistency at each time step.

Table 2-2. Air Species Components [A_i]

No.	Species		No.	Species
1	H_2O		21	NO_2
2	H_2O_2		22	NO_3
3	$\cdot H$		23	N_2O
4	$\cdot OH$		24	HNO_2
5	$\cdot HO_2$		25	HNO_3
6	H_2		26	NH
7	O_2		27	NH_2
8	$\cdot O$		28	NH_3
9	O_3		29	N_2O_5
10	O_2^-		30	NH_4NO_2
11	O_2^+		31	NH_4NO_3
12	O^+		32	NO_2^-
13	H_2O^+		33	N_2^+
14	H_3O^+		34	NO^+
15	e^-		35	N^+
16	N_2		36	CO_2
17	$\cdot N$		37	CO
18	$N(^2D)$		38	CO^+
19	$N(^4S)$		39	CO_2^+
20	NO		40	He

A listing of the FORTRAN program is given in Appendix B.

2.2 Model Verification

Model testing was performed during the radiolysis model development. The reactions modeled for water vapor radiolysis were reproduced from a radiolysis model of water vapor in the first-loop coolant for boiling water-moderated, water-cooled nuclear reactor facilities (Arkhipov et al. 2007). That work reported calculations of radiolytic H_2 production in the temperature range 450-900 K, dose rates 500-3x10^{11} Gy/sec, and vapor density 0.25-1 g/L. The current model could reproduce all numerical results of that work to the accuracy reported. Figure 2-1 gives an example where the calculated H_2 yield with time is visually identical with the curves of Fig. 1 of Arkhipov et al. (2007). Additionally, in reproducing Table 2 of Arkhipov et al. (2007), it was discovered that the calculations should refer to 5-ns pulses rather than the mistyped 0.5-ns stated in the caption.

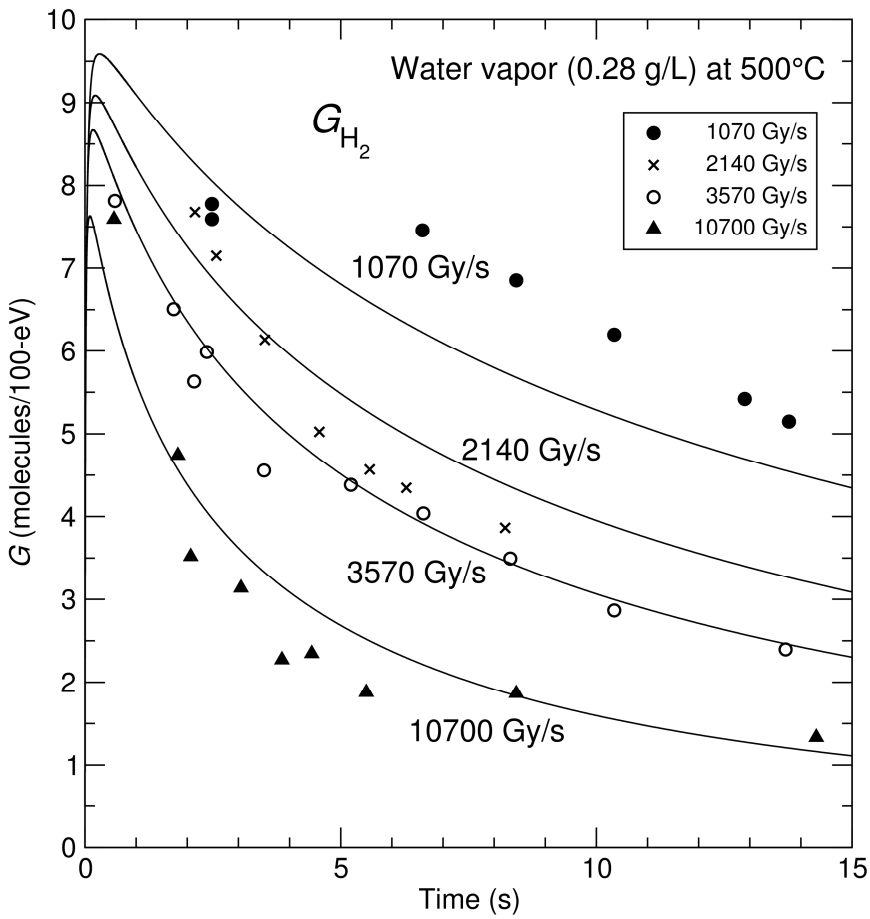

Figure 2-1. Hydrogen Yield as a Function of Irradiation Time for Water Vapor at 773 K Calculated to Confirm that the Radiolysis Model Here Could Reproduce the Model Results of Arkhipov et al. (2007) Data is from Dzantiev et al. (1984)

In addition to comparing with independent model results, the model solution consistency was tested for atom and charge balance over 200,000 time steps for a 300-year concentration history.

3. SENSITIVITY OF RADIOLYSIS TO CANISTER ENVIRONMENT

Given the limited data and uncertainties for the temperature, dose rate, and gas composition inside the canister fill gas and external to the canister, model calculations are performed over various conditions that are expected to be representative of a typical storage canister.

3.1 Canister Fill Gas

The canister drying process includes vacuum drying and backfilling the free volume with helium gas at approximately 5-atm in some vertical designs for increased thermal conductivity. A literature review on sources of residual water along with uncertainties in incomplete drying indicates a range of 1 to 5 moles of remaining water (Ahn et al. 2013).

The nominal dose rate inside the canister is assumed to be the gamma dose rate outside pressurized water reactor spent nuclear fuel (SNF) rods (Table 3-1). The dose rates are taken from Bechtel SAIC Company (BSC 2002, Tables 15 and 17).

Table 3-1. Gamma dose rates outside Pressurized Water Reactor Spent Nuclear Fuel Rods. Table reproduced from BSC (2002)

Age (Years)	Dose Rate at Relative Humidity 40%, Temperature 90°C (R/hr)	Dose Rate at Relative Humidity 90%, Temperature 90°C (R/hr)
10	7.81×10^4	7.82×10^4
15	5.75×10^4	5.76×10^4
20	4.69×10^4	4.69×10^4
25	4.02×10^4	4.02×10^4
35	3.04×10^4	3.04×10^4
50	2.10×10^4	2.10×10^4
70	1.31×10^4	1.31×10^4
100	6.51×10^3	6.50×10^3
150	2.05×10^3	2.05×10^3
200	6.46×10^2	6.46×10^2
250	2.07×10^2	2.07×10^2
350	2.52×10^1	2.52×10^1
500	5.54	5.54
700	4.65	4.65
1,000	4.29	4.29
1,500	4.07	4.07
2,000	3.83	3.83
2,500	3.75	3.75
3,500	3.65	3.65
5,000	3.52	3.52
7,000	3.39	3.39
10,000	3.24	3.24

Neutron dose rates are roughly four orders of magnitude lower than gamma dose rates for the time period shown in Table 3-1 (BSC 2002). Doses are from the central nine SNF assemblies and were calculated using the Monte Carlo N-Particle (MCNP) software code. The pressurized

water reactor SNF assembly used in the calculation was a Babcock and Wilcox 15-by-15 assembly, and it was assumed to have 4.0 wt% initial ^{235}U, 48 GWd/MTU burnup, and 21-year decay time (BSC 2002, 2004).

A fit to the Table 3-1 values is used in the model (see Figure 3-1) where the dose rate $\dot{d}$ is given as a function of time in years. Figure 3-1 also shows a typical central zone temperature (Suffield et al. 2012 and Ahn et al. 2013) of the canister where the final temperature (T_∞) is assumed to be 37°C and the decay rate is based on a 30-year half-life.

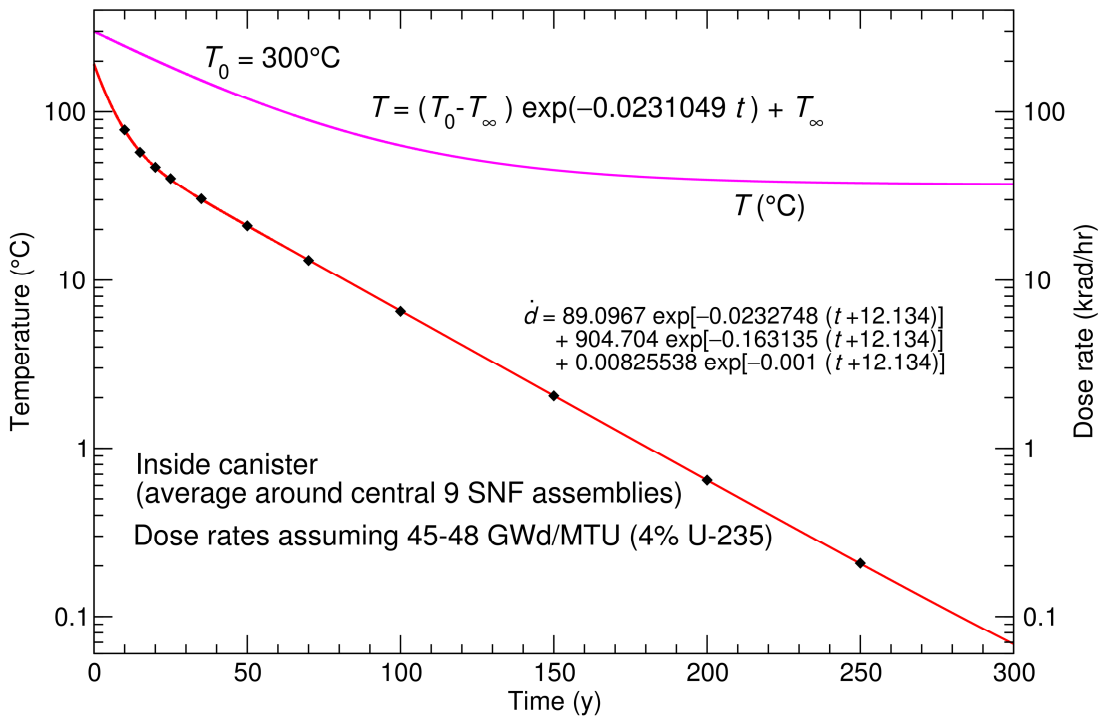

Figure 3-1. Dose Rate and Cooling History fit to BSC (2004)

Given the dose rate history of Figure 3-1 and a G-value for water of –7.35 molecules/100-eV (Table 2-1), the black-dashed curve of Figure 3-2(b) shows the fraction of water depleted by radiolysis, assuming no reaction kinetics. Full kinetics results indicate that this assumption is bounding. In this case, the reaction kinetics of Eq. (1) decouple to give a simple solution to the water rate equation in terms of the integrated dose:

$$M_{\mathrm{H_2O}}(t) = M_{\mathrm{H_2O}}(0)\exp\left[-\left|G_{\mathrm{H_2O}}\right| w_{\mathrm{H_2O}} \int_0^t \dot{d}(t)\,dt\right] . \tag{3}$$

The solid curves of Figure 3-2 (b) show the effect of reaction kinetics for 55 moles of water vapor in the 4500 L of free space in an approximately 70-in.-diameter fuel container for the temperature histories shown on the left-side (Figure 3-2a). The temperature histories are typical for a 180-in.-high canister center Zone-1 (Figure 3-2, magenta) and outward zones from the center (Figure 3-2, red to blue) (Ahn et al. 2013). The model indicates that a helium fill gas with

no air contamination goes rapidly to a steady state where the recombination of radiolysis products dominates to give less than 10 ppm levels of H_2 and O_2. For almost any level of air contamination, reaction pathways are opened that effectively compete with recombination leading to a few percent levels of H_2 with oxygen bound in nitrogen compounds. While neglecting reaction kinetics is in most cases extremely conservative, even small fractions (few percent) of air can increase the fraction of water radiolysis toward the pure G-value estimate with increased H_2.

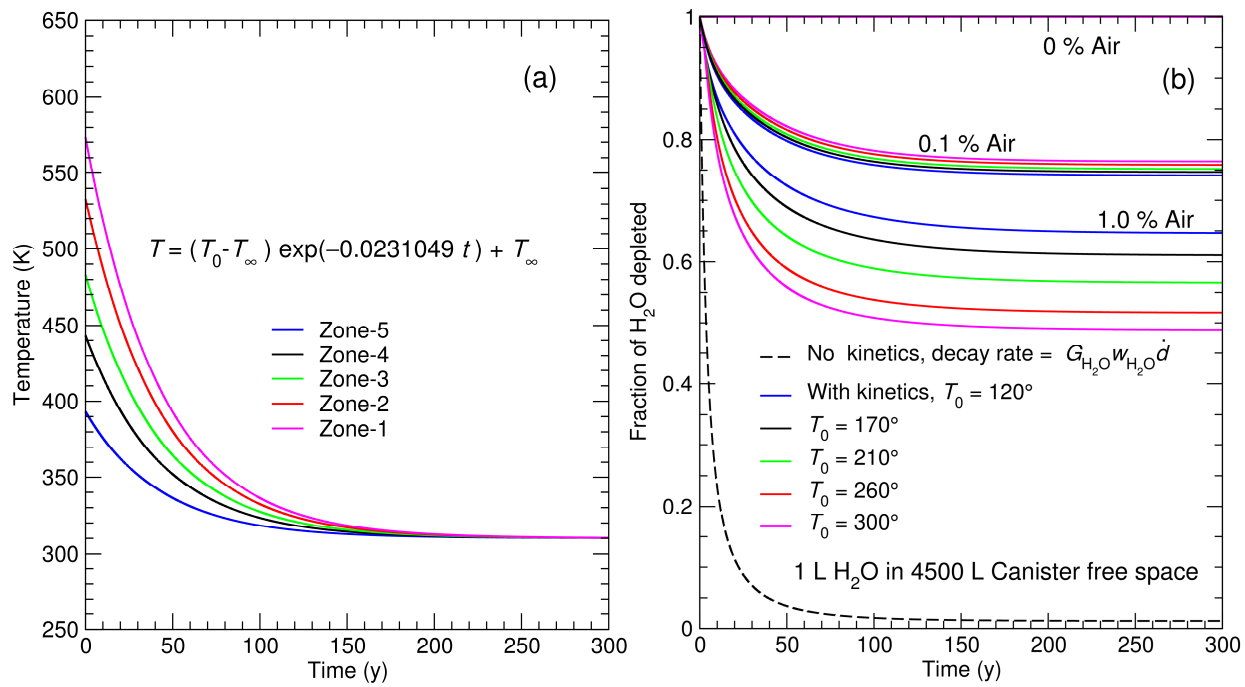

Figure 3-2. (a)Typical Canister Temperature Histories, (b) with the Effect of Temperature and Air in the Helium Fill Gas on Water Radiolysis

For very low concentrations of air (0.1%) the temperature effects tend to be small where recombination kinetics are accelerated at increasing temperature which slightly reduce the depletion of water. At higher air concentration (1%) the effect is greater and reverses because radiolytic products containing oxygen react more rapidly with N_2 to form nitrogen compounds like HNO_3 rather than recombining with hydrogen. Gas survey data from the Idaho National Engineering and Environmental Laboratory (Bare and Torgerson 2001) show N_2 concentrations typically at about 2% and lower and at much higher concentrations for samples assumed to have been contaminated. It was considered very unlikely that air could leak into a pressurized canister to give 30% and higher N_2 concentrations, while not unlikely that a percent of N_2 could remain during the filling procedure. Figure 3-3 shows the gas composition details corresponding to the highest and lowest temperature zones of Figure 3.2(a) with 1 L of residual water and 1% air over 16 years—the concentration levels assume a helium backfilling pressure of 5 atm. With no air present (dashed line in Figure 3-3), the H_2 and O_2 concentrations rapidly reach a steady-state that

follows the dose rate curve. With 1% air (solid curves in Figure 3-3), it is seen that O_2 depletion allows for the increased H_2 and HNO_3 concentrations.

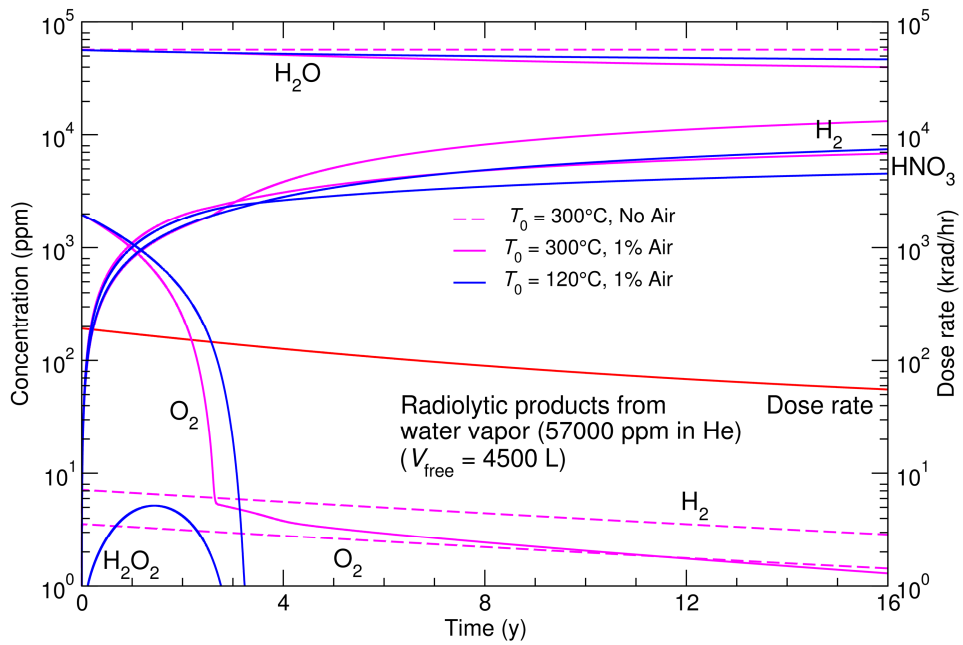

Figure 3-3. Fill Gas Composition Assuming 1 L Water and 1% Air (Solid Line) and No Air (Dashed Line)

This model result shows that sample gas containing approximately 1% N_2 should be depleted in O_2 after only a few years, which is not the seen in the data, indicating that the model is not correct, that sampling process was prone to some air contamination before analysis, or that the assumed conditions (e.g., 1 L residual water) are not representative. Since none of the fill gas data show H_2 levels as high as 1% as in Figure 3-3, it is likely that the modeled conditions are conservative. The 1 L (55 moles) of residual water is considered to be 10 times greater than the amount expected from a properly executed vacuum drying procedure (ASTM 2008 and Ahn et al. 2013). Additionally, even 1% of air is likely to be much higher than expected for a standard helium purge and filling operation. Even under these conditions, the highest concentration of H_2 is about 2.3% (Figure 3-4). The dashed lines of Figure 3-4 show the effect of a reduced dose rate and initial temperature from assuming an additional 10-year delay on canister filling. The effect of a 10-year delay is more than a simple concentration shift in time because of the nonlinear kinetics. Figure 3-4 shows that the steady-state H_2 concentration is reduced to about 1.6%.

At a reduced initial air concentration of 0.1% the O_2 depletion does not occur for the 1 L residual water case (Figure 3-5), but does still occur for 0.2 L of remaining water (Figure 3-6). The latter case seems to be the most consistent with previous fill gas data (Bare and Torgerson 2001, McKinnon and Doherty 1997), specifically the observed levels of H_2 and the depleted O_2 for cases with low N_2 (< 1%)—data with higher levels of N_2 would then be interpreted as air-contaminated samples.

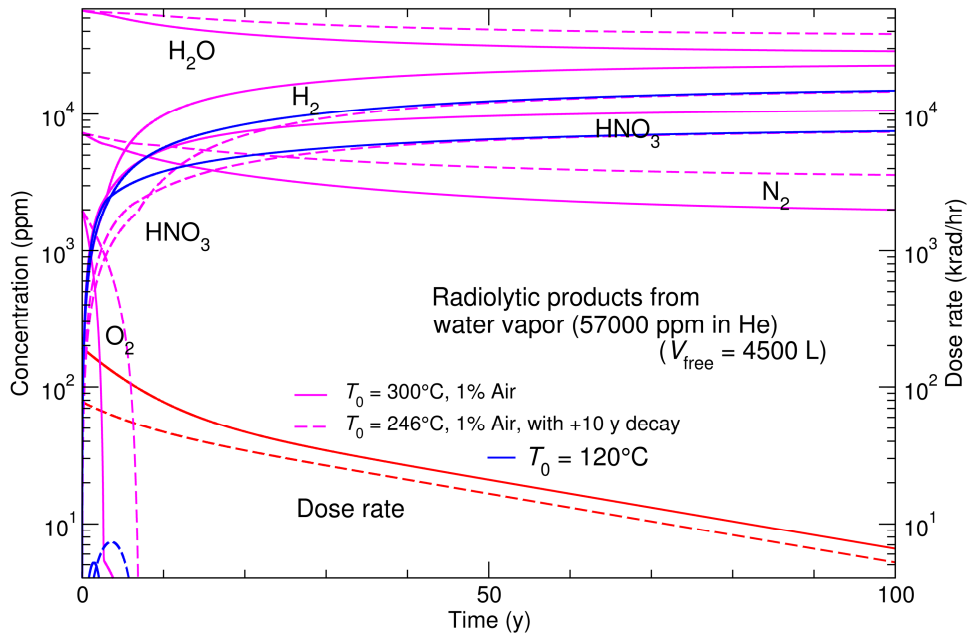

Figure 3-4. Fill Gas Composition over 100 Years Assuming Residual 1 L of Water and 1% Air with Nominal Dose Rate (Solid Line) and with an Additional 10-Year Decay (Dashed Line)

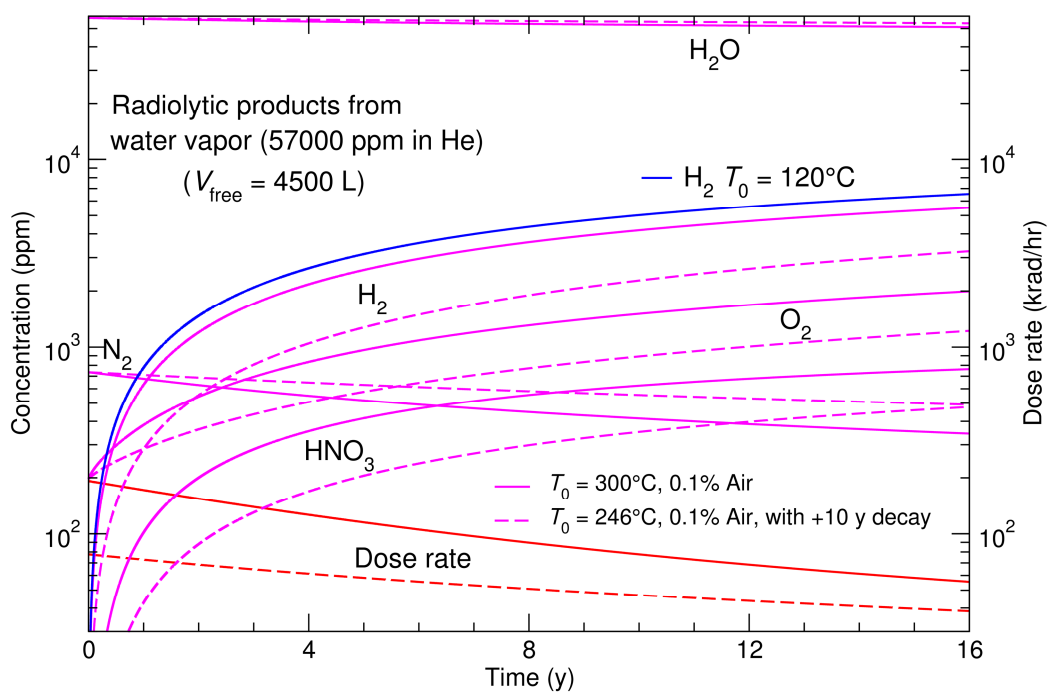

Figure 3-5. Fill Gas Composition Assuming Residual 1 L of Water and 0.1% Air with Nominal Dose Rate (Solid Line) and with an Additional 10-year Decay (Dashed Line)

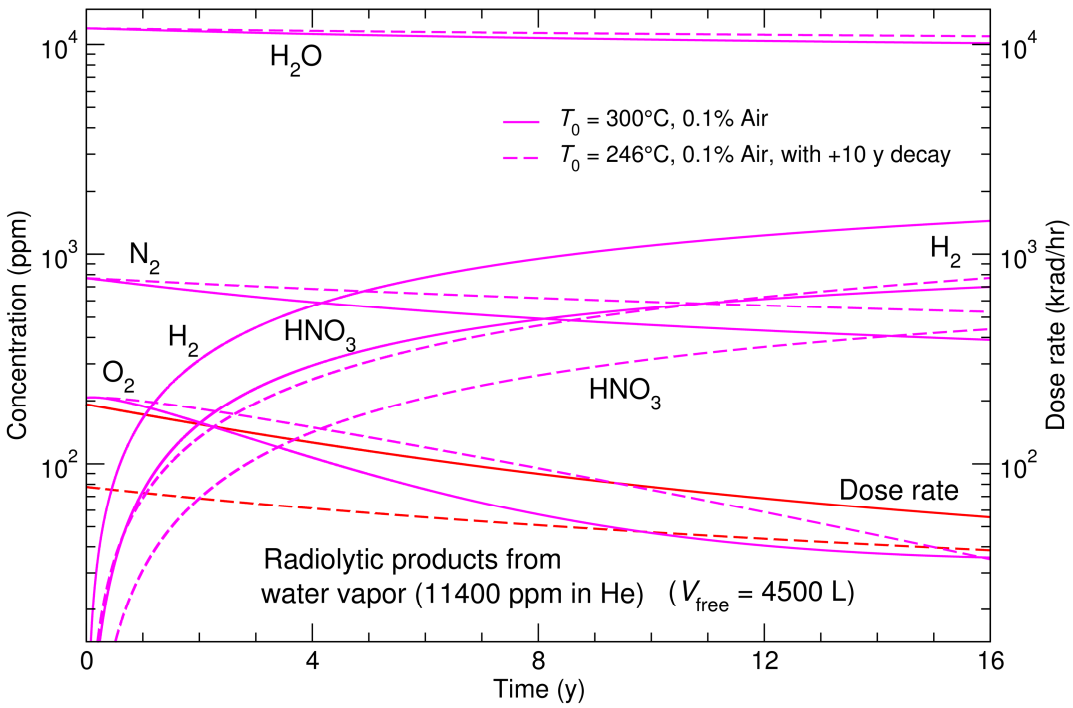

Figure 3-6. Fill Gas Composition Assuming Residual 0.2 L of Water and 0.1% Air with Nominal Dose Rate (Solid Line) and with an Additional 10-year Decay (Dashed Line)

Figure 3-7 shows the radiolysis products for the same case out to 150 years where after 50 years O_2 is generated rather than consumed by radiolytic-induced reactions with N_2. Tables 3-2 to 3-6 give gas compositions at 16 and 300 years for the highest and lowest temperature zones.

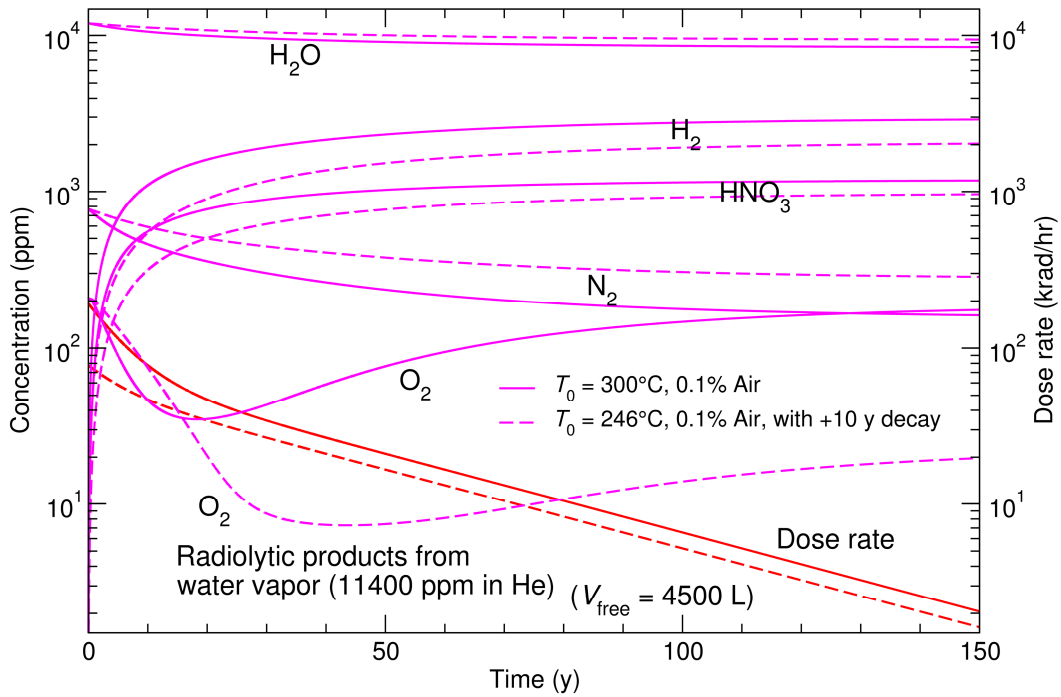

Figure 3-7. Fill Gas Composition Assuming Residual 0.2 L of Water and 0.1% Air with Nominal Dose Rate (Solid Line) and with an Additional 10-year Decay (Dashed Line)

Table 3-2. Fill Gas Composition Assuming 1 L Water at 16 Years

	1% Air				0.1% Air			
T_0(°C)	H_2	O_2	N_2	HNO_3	H_2	O_2	N_2	HNO_3
120	0.746	0.000	0.501	0.455	0.654	0.251	0.034	0.077
300	1.315	0.000	0.388	0.683	0.550	0.199	0.034	0.076

Table 3-3. Fill Gas Composition Assuming 1 L Water at 300 Years

	1% Air				0.1% Air			
T_0(°C)	H_2	O_2	N_2	HNO_3	H_2	O_2	N_2	HNO_3
120	1.606	0.000	0.330	0.799	1.382	0.562	0.013	0.119
300	2.347	0.000	0.182	1.096	1.254	0.498	0.013	0.119

Table 3-4. Fill Gas Composition Assuming 0.1 L Water at 16 Years

	1% Air				0.1% Air			
T_0(°C)	H_2	O_2	N_2	HNO_3	H_2	O_2	N_2	HNO_3
120	0.318	0.000	0.569	0.264	0.072	0.010	0.046	0.030
300	0.378	0.000	0.553	0.285	0.074	0.002	0.046	0.040

Table 3-5. Fill Gas Composition Assuming 0.1 L Water at 300 Years

	1% Air				0.1% Air			
T_0(°C)	H_2	O_2	N_2	HNO_3	H_2	O_2	N_2	HNO_3
120	0.420	0.000	0.509	0.281	0.149	0.016	0.026	0.053
300	0.431	0.000	0.490	0.275	0.151	0.001	0.030	0.072

Table 3-6. Fill Gas Composition Assuming 0.2 L Water at 0.1% Air

	16 years				300 years			
T_0(°C)	H_2	O_2	N_2	HNO_3	H_2	O_2	N_2	HNO_3
120	0.142	0.003	0.039	0.070	0.295	0.019	0.016	0.119
300	0.144	0.004	0.039	0.070	0.296	0.019	0.016	0.119

The case of 1 L residual water and 1% air show the greatest H_2 and HNO_3, about 2.3% and 1.1% respectively. The highest O_2 concentrations (approximately 0.5%) occur for cases with 0.1% air because radiolytic reactions with N_2 consume O_2. These relationships among the radiolytic products can also be seen in the composition correlation matrices in Tables 3-7 to 3-9. While different conditions can lead to very different gas composition time histories, the correlation between species at 16 years and 300 years is very similar. As expected, correlations with H_2O (both +/–) increase with time and O_2 is negatively correlated with N_2 and HNO_3.

Table 3-7. Composition Correlation Matrix at 16 Years

Comp.	H_2O	H_2	O_2	N_2	HNO_3
H_2O	1.000	0.742	0.684	-0.018	0.356
H_2	0.742	1.000	0.255	0.459	0.851
O_2	0.684	0.255	1.000	-0.340	-0.260
N_2	-0.018	0.459	-0.340	1.000	0.759
HNO_3	0.356	0.851	-0.260	0.759	1.000

Table 3-8. Composition Correlation Matrix at 300 Years

Comp.	H_2O	H_2	O_2	N_2	HNO_3
H_2O	1.000	0.801	0.747	-0.206	0.362
H_2	0.801	1.000	0.354	0.139	0.816
O_2	0.747	0.354	1.000	-0.330	-0.245
N_2	-0.206	0.139	-0.330	1.000	0.429
HNO_3	0.362	0.816	-0.245	0.429	1.000

Table 3-9. Composition Correlation Matrix (All)

Comp.	H_2O	H_2	O_2	N_2	HNO_3
H_2O	1.000	0.641	0.607	-0.077	0.313
H_2	0.641	1.000	0.370	0.185	0.823
O_2	0.607	0.370	1.000	-0.315	-0.206
N_2	-0.077	0.185	-0.315	1.000	0.505
HNO_3	0.313	0.823	-0.206	0.505	1.000

The concentration of H_2O_2 for gas phase radiolysis was found to be negligible (< 10-ppm) for all the conditions considered. While the corrosion impact may be negligible as compared with the O_2 and HNO_3 concentrations, the possibility of H_2O_2 formation in a thin layer of water on surfaces should be considered. A water radiolysis model developed for UFD degradation modeling (Wittman and Buck 2012) was used to calculate water radiolysis assuming the dose rate and temperature environment of the canister fill gas. The Eq. 1 rate equations were solved with Table 3-10 aqueous species and G-values. The reactions considered are given in (Wittman and Buck 2012), where the only temperature dependence considered was for H_2O_2 decomposition where $k_d = 10^{-3}$ s^{-1} at 280°C with an activation energy $E_a = 4930$ K.

Table 3-10. Gamma Dose G-values for Liquid Water

Species	G (particles/100-eV)
H^+	3.10
OH^-	0.50
H_2O	-4.64
H_2O_2	0.70
HO_2^-	0.00
e_{aq}^-	2.60
$\cdot H$	0.66
$\cdot OH$	2.70
O^-	0.00
$\cdot HO_2$	0.02
O_2^-	0.00
O_2	0.00
H_2	0.45
$\cdot O$	0.00

Figure 3-8 shows that H_2O_2 concentration is primarily sensitive to the initial dissolved O_2 concentration. With no initial O_2 the H_2O_2 concentration is less than 1 μM over 300 years with very little temperature sensitivity because H_2O_2 destruction is controlled by reactions with short-lived radicals rather than thermal decomposition. For higher concentrations of dissolved O_2 that could originate from water vapor radiolysis or initial residual air, the H_2O_2 increases because O_2 competes for the same radicals that react with H_2O_2 and allows thermal decomposition to be the limiting effect for earlier years.

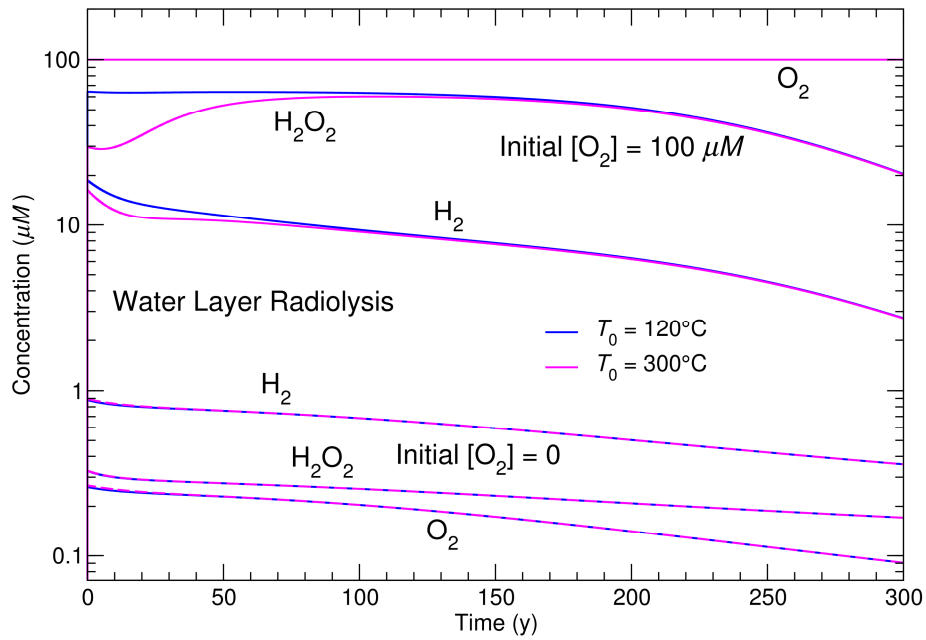

Figure 3-8. Concentrations of Water Layer Radiolysis Products as a Function of Time

The H_2O_2 concentration for T_i = 300°C (magenta curve) is about one-half the concentration for T_i = 120°C (blue curve) for the first 30 years, although it should be mentioned that at 5-atm water condenses at about 150°C (Engineering Tool Box 2013*)*. At 25°C and atmospheric partial pressure of O_2, the O_2 solubility is about 300 *μM,* which should be much greater than the concentrations expected in residual liquid water. Therefore, the 60-70 *μM* range (Figure 3-8, $[O_2]$ = 100-*μM*) is likely to be an upper bound for H_2O_2 dissolved in water on structural surfaces. In the future, a more consistent assessment could be made with a coupled liquid-gas radiolysis model.

3.2 Hydrogen Generation

To focus more directly on the issue of H_2 generation inside a canister, Figure 3-9 shows the H_2 concentration assuming 1 L of residual water for T_i = 300°C with reaction kinetics (magenta and violet curves) and with no reaction kinetics (black curves) – the solid black curves here correspond to the black curve of Figure 3-2(b). For the no kinetics case, the 4% flammability limit is reached in about 8 years and in about 23 years assuming a lower initial dose rate from an additional 10 year decay. This result was found to be bounding for all fill gas conditions that included reaction kinetics. The 4% limit was not reached for the case that included reaction kinetics with 1% residual air (Table 3-3). In the case of 10% residual air the H_2 concentration approached close to 4% in about 14 years and in about 33 years for the lower dose case. A possible question for the more plausible 1% residual air case is: What amount of residual water would be required to reach the flammability limit? While it is possible that the model results are outside the range of applicability for very high concentrations of water vapor or even likely that

the form of water and water vapor is not physical, the model predicts that 20 L of water would be required to reach the 4% H_2 flammability limit in 16 years, and between 3 and 4 L of water to reach the 4% H_2 flammability limit in 300 years.

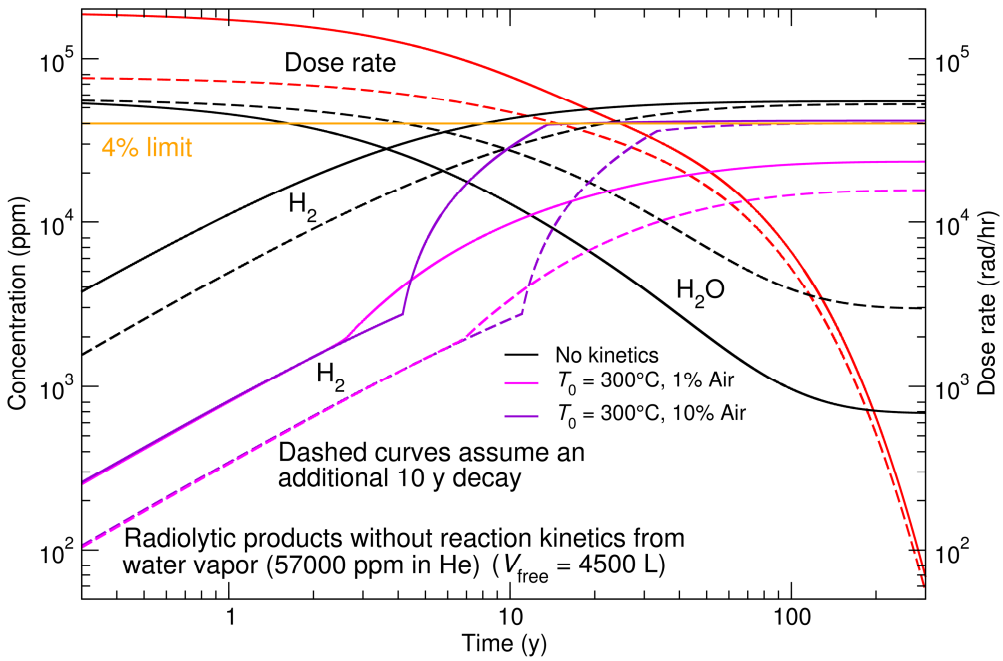

Figure 3-9. H_2 Concentration as a Function of Time Comparing the Effect of Reaction Kinetics (magenta & violet curves) with the no Kinetics result (black curves).

3.3 External Canister Air

External air flows between the outer canister walls and the external concrete cask shielding. The convective air flow in this region is necessary for cooling the canister. A fit to a typical external dose rate just outside the canister is shown Figure 3-10 along with the inside dose rate of Figure 3-1 for comparison.

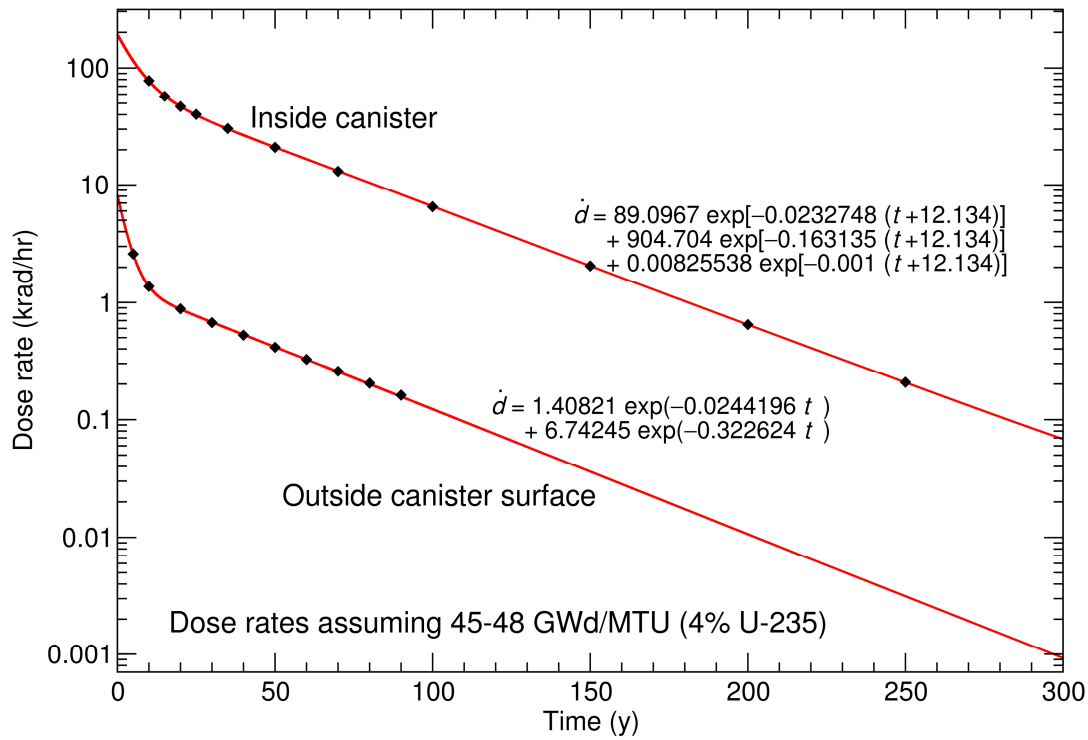

Figure 3-10. Comparison of Fits to Inner and Outer Canister Dose Rate Histories

For this study, the dose rate fit of Figure 3-10 is assumed as the nominal dose rate to the air flowing past the canister surface as well as any layer of liquid water on the outside surface. Cases were considered with an additional 5-year decay to assess the sensitivity to dose rate. Air temperature was considered constant over the storage history and it was determined that the gas composition was relatively insensitive to temperature (25-50°C). The air flowing into the radiation field around the canister was atmospheric pressure air with various amounts of moisture. The moisture content of the air did have an effect primarily on the partitioning of the radiolytically produced nitrogen containing gases, but even without water vapor, NO_X compounds were formed from the presence of N_2 and O_2 and their radiolytically induced reactions. Additionally, CO was produced from atmospheric CO_2. Table 3-11 gives the air composition (Railsback 2013) assumed for $[A_i]_0$ of Eq. (1) for 100% relative humidity (RH) air at 20°C and at 37°C. In this temperature range the moisture content of saturated air changes by more than a factor of two.

Table 3-11. External Air Composition at 100% Relative Humidity

	20°C	37°C
Species	Conc (ppm)	Conc (ppm)
N_2	7.698×10^{5}	7.427×10^{5}
O_2	2.065×10^{5}	1.992×10^{5}
H_2O	2.332×10^{4}	5.766×10^{4}
CO_2	3.923×10^{2}	3.785×10^{2}
H_2	5.939×10^{-1}	5.730×10^{-1}
N_2O	3.508×10^{-1}	3.385×10^{-1}
CO	1.080×10^{-1}	1.042×10^{-1}
O_3	3.780×10^{-2}	3.647×10^{-2}
NO_2	2.160×10^{-2}	2.084×10^{-2}

The following figures show model results for how the composition of air in the radiation field outside the canister changes with time under various conditions: the time-scale is from 0.1 days out to 300 years.

Figures 3-11 and 3-12 show the highest radiolytic products generated in air with 100% RH at 20°C and at 37°C (Table 3-11). The temperature change was found to be a small effect on kinetics—the main difference is the higher moisture content (> 2X) at the greater temperature for 100% RH. Three effective flow conditions are considered in the figures by assuming 1) a fixed air residence time (dashed curve), 2) a residence time that increases to 100 days as the dose rate goes to zero (solid curve), and 3) a residence time that increases to 1000 days as the dose rate goes to zero (dash-dotted curve). Both the 100-day and 1000-day final residence time cases are very conservative with the 1000-day case approaching a closed system. The purpose of considering the long times is not to accurately model the flow history, but to understand the affect that reduced flow conditions have on air composition. Consistent with a simple continuous stirred tank reactor (CSTR) analysis, the maximum concentrations are closely proportional to the initial residence time (Figures 3-12 to 3-16). The effect of increasing the final resident time (effectively a reduced flow) with cooling is to sustain the maximum concentrations as the dose rate decreases with time. For air resident times that are consistent with cooling studies (Suffield et al. 2012) all radiolytic product concentrations are less than 1-ppm (Figure 3-16). This seems to indicate that corrosive oxidants generated in the air are likely to have little or no impact on the canister surface.

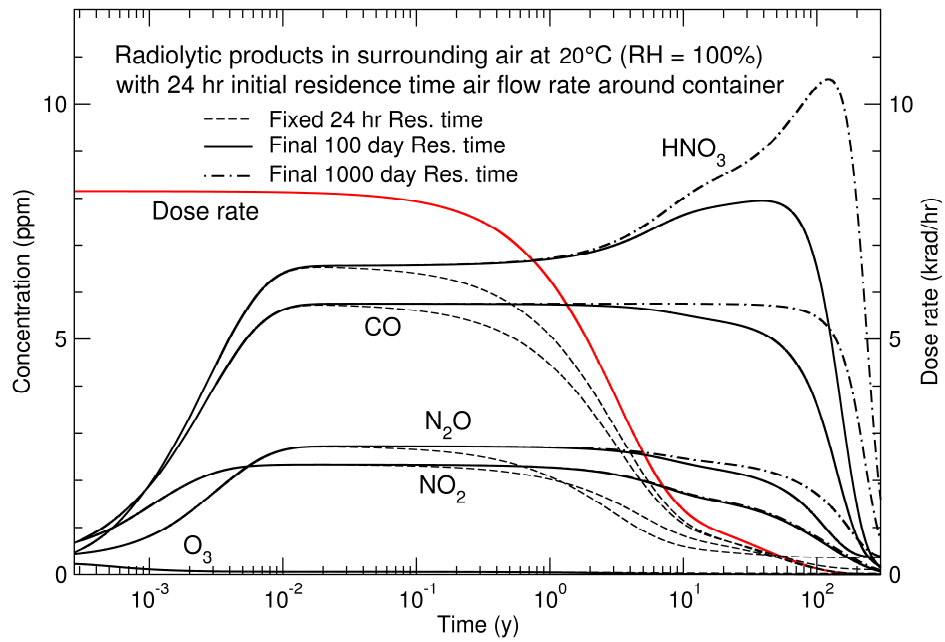

Figure 3-11. External Air (at 20°C) Radiolysis Product Concentration as a Function of Time

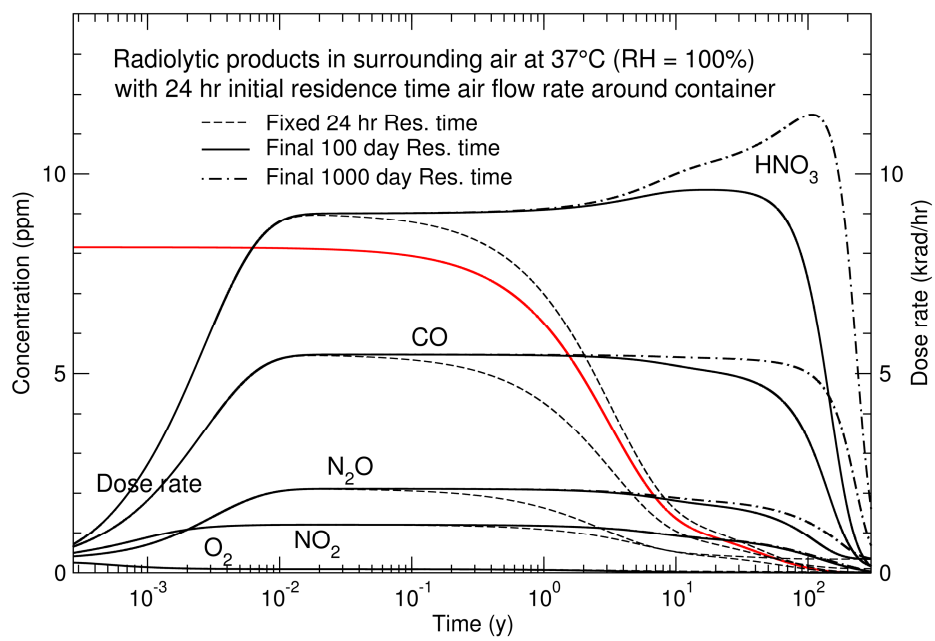

Figure 3-12. External Air (at 37°C) Radiolysis Product Concentration as a Function of Time

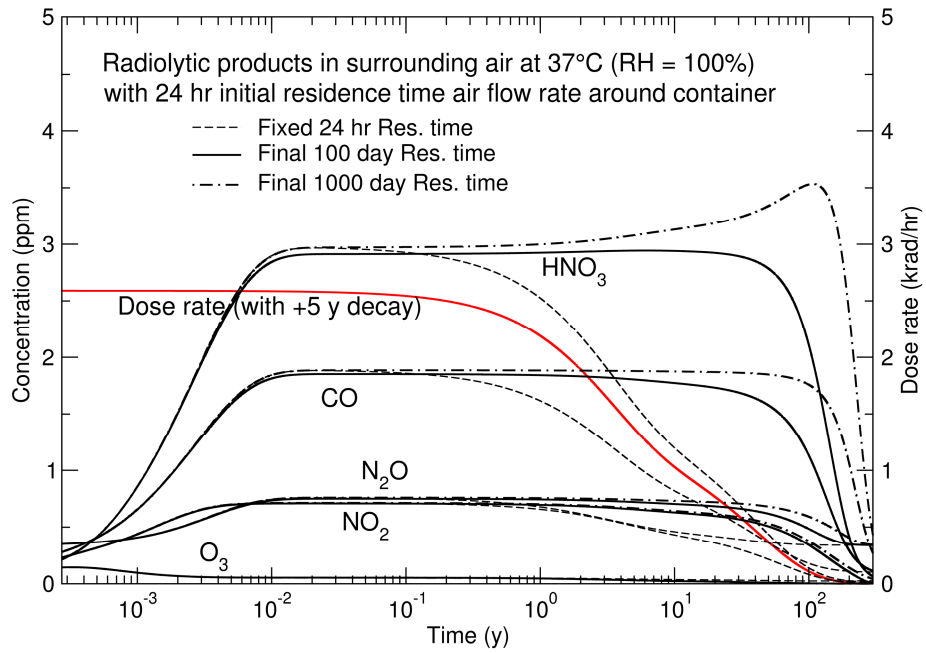

Figure 3-13. External Air Radiolysis Product Concentration as a Function of Time with Reduced Dose Rate from Assuming an Additional 5-year Decay

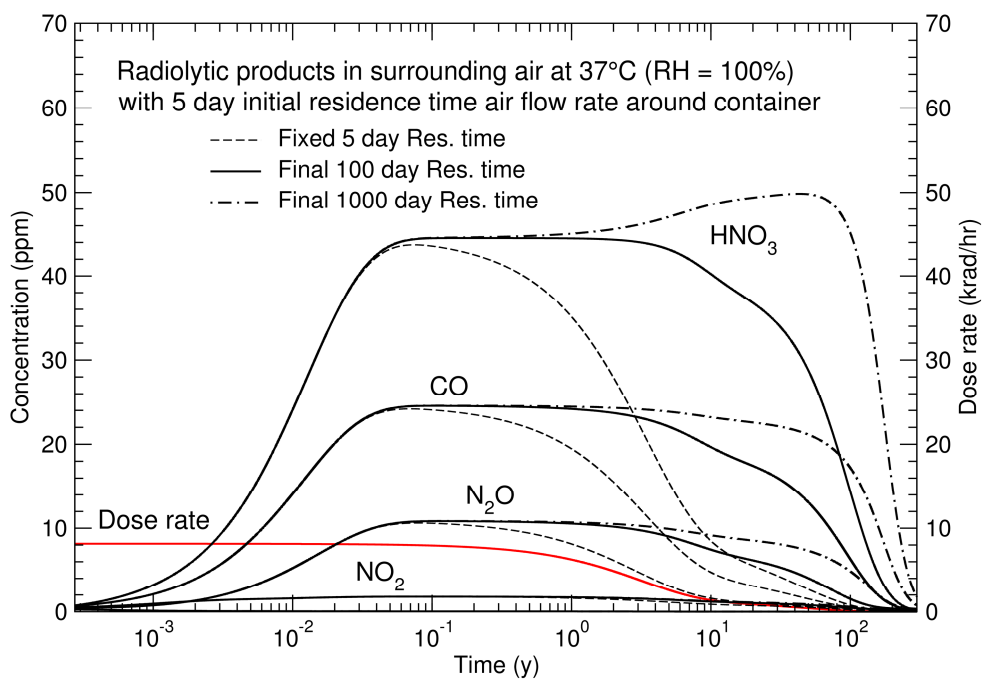

Figure 3-14. External Air Radiolysis Product Concentration as a Function of Time Assuming an Initial 5-day Air Residence Time

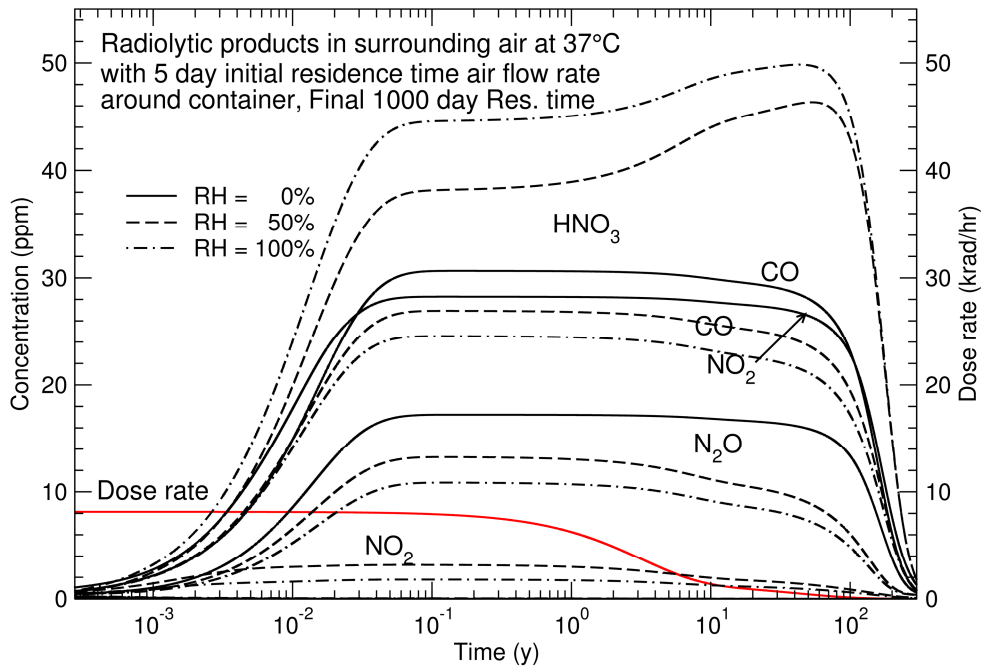

Figure 3-15. External Air Radiolysis Product Concentration as a Function of Time at a Relative Humidity of 0% (Solid Curves), 50% (Dashed Curves) and 100% (Dash-dotted Curve)

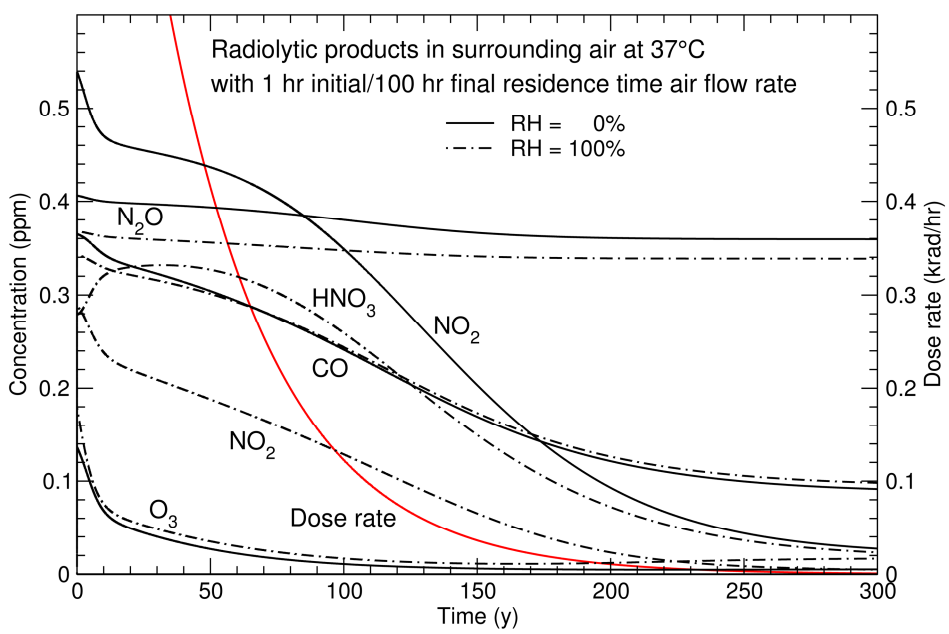

Figure 3-16. External Air Radiolysis Product Concentration as a Function of Time at a Relative Humidity of 0% (Solid Curve) and 100% (Dash-dotted Curve) for Air Residence Times Consistent with Cooling Studies

As in the case of the fill gas, no significant amount of H_2O_2 was predicted in the air because reactions producing nitrogen compounds dominated. Assuming that the actual corrosion processes occur in a thin film of liquid water on the canister surface, the radiolytic production of H_2O_2 was calculated (Figure 3-17) for liquid water with the G-values of Table 3-10 and the dose rate curve of Figure 3-10 (solid curves of Figure 3-17) and with an additional 5-year decay (dashed curves of Figure 3-17). In this case, the atmospheric dissolved O_2 was assumed to be 300 μM at 25°C (298 K) and is approximated by Henry's Law according to Battino and Clever (1966)

$$[\mathrm{O_2}] = (300\mu M)\exp\left[-1700\ \mathrm{K}\left(\frac{1}{T} - \frac{1}{298\ \mathrm{K}}\right)\right] \tag{4}$$

for any surface temperature T in Kelvin. The higher dose rate solid curves of Figure 3-17 show that both thermal decomposition and radical destruction of H_2O_2 influence the peak concentration. While thermal decomposition is greater at 50°C than at 37°C, the increased solubility of O_2 reduces the radical concentration to favor a higher (approximately 0.25 mM) H_2O_2 concentration. At 100°C thermal decomposition dominates to lower the H_2O_2 concentration. For t greater than 10 years and for the additional 5-year decayed lower dose rate cases, thermal decomposition has the greatest influence, H_2O_2 concentration is lowered with increased temperature. At 100 years all cases show H_2O_2 concentrations at about 30 to 40 μM which fall to less than 1 μM at 300 years.

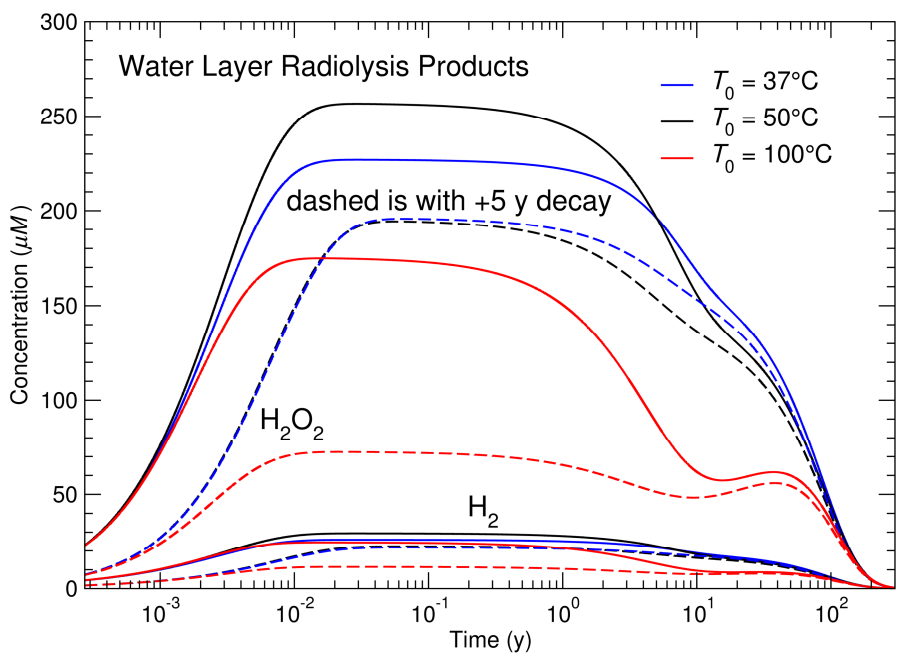

Figure 3-17. Temperature Dependence of Liquid Water Layer Radiolysis Products as a Function of Time with Nominal Radiation Field (Solid Curves) and with Additional 5-year Decay (Dashed Curves)

4. DISCUSSION AND FUTURE WORK

This section summarizes the previous radiolysis model results for conditions inside and outside the canister and notes results that could be significant with regard to canister integrity. Future work is suggested to verify the model and to highlight model limitations that could be removed with further development.

4.1 Radiolysis in Canister Fill Gas

In addition to the helium fill gas, a canister was considered to contain a range of residual water and air at various temperatures. The primary radiolysis products were H_2, O_2, and HNO_3. Without the presence of residual air, water radiolysis products rapidly recombine and persist at very low concentrations (< 10 ppm), even with 55 moles of residual water. Of course this does not account for the effect of surface reactions competing with recombination. It was determined that even small amounts of residual air (approximately 0.1 %) enable reactions that effectively compete with recombination to greatly increase the generation of radiolysis gases. The greatest temperature dependence was seen for greater concentrations of residual air because of the increased rates of radiolytically induced reactions with N_2, which are favored over recombination. At lower N_2 concentrations (approximately 0.1%), the temperature dependence is small and the effect reverses because higher temperature also increases the rate of recombination reactions. While there are large data uncertainties, fill gas data for storage times of 10-16 years was not inconsistent with model results assuming residual water and air of about 0.2 L and 0.1% respectively, where approximately 0.2% H_2 and air depleted in O_2 were observed. The model predicts initial O_2 depletion for this case and O_2 generation for times greater than 50 years when N_2 concentration is reduced. While levels of H_2, O_2, and HNO_3 were less than 1% for this case, even at 300 years, greater amounts of residual water resulted in H_2 and HNO_3 concentrations of slightly greater than 1%. In the case of 1 L of residual water, H_2 concentration reached 2.3% in 300 years. Previous work (Sunder and Miller 1996) observed NO_2 generation in irradiated (presumably dry) air. While the O_2 concentration is likely to be small in the fill gas, it has been noted that the presence of nitrogen oxide at 1.0% increases the oxidation rate for UO_2 and should be included in detailed models of fuel oxidation (McEachern et al. 1998). Model results also indicated that H_2O_2 is produced at only very low concentrations (< 10 ppm) in the fill gas, but is the major radiolysis product in liquid water, and could reach 10-100 μM levels in liquid water layers on surfaces.

4.2 Radiolysis Outside Canister Surface

The space between the outside canister surface and inside the concrete shielding was assumed to contain air of various moisture contents defined by outside air conditions. The effect of temperature on gas radiolysis was primarily related to the external air saturation moisture content with only a small effect on the kinetics. Air residence times were applied to determine the effect of air flow and stagnant air conditions on radiolysis products. The main radiolysis products HNO_3, CO, N_2O, and NO_2 attained levels of 10-50 ppm with O_3 as high a 0.25 ppm. As expected, moist air favored HNO_3 production and dry air favored NO_2 production. For greater flow conditions consistent with cooling studies, all radiolysis product concentrations were less

than 1 ppm. As in the case of the fill gas, only trace levels of H_2O_2 are produced in the outside air, but could reach 0.05-0.2 m*M* concentrations in liquid water on the canister surfaces. The H_2O_2 concentrations showed a strong temperature dependence in the liquid water because both thermal decomposition and the temperature-dependent O_2 solubility affect the main H_2O_2 removal mechanisms.

4.3 Future Work

While the results of this work indicate low concentrations of all gas radiolysis products outside the canister and sufficiently low concentrations (< 4%) of H_2 inside the canister, a more direct comparison of model results with canister data would give greater confidence in model predictions. It would be beneficial to collect fill gas data from a canister with a known thermal and dose rate history. Even without fill gas data, monitoring the outlet cooling air for ppm levels of radiolysis gases under known canister conditions could refine modeling assumptions.

Additional model refinements include consistently coupling the radiolytic effects for water vapor with liquid water. For example, generation of O_2 in the fill gas that dissolves into liquid water could strongly increase H_2O_2 production in the water. It also should be determined how the steady state and bounding concentrations are affected by accounting for reactions of radiolytic products with exposed surfaces. If the concentrations reported here are considered to be great enough to expect significant surface oxidation, future work could develop a comprehensive model (as suggested by Ahn et al. 2013) that couples gas and liquid phase radiolysis with the electrochemical oxidation of cladding and exposed UO_2.

5. REFERENCES

Ahn T, H Jung, PK Shukla, EL Tipton, and K Das. 2013. "Extended Dry Storage and Transportation: Model for Evaluating Vacuum Drying Adequacy," Presented at the 2013 International High-Level Radioactive Waste Management Conference (IHLRWMC) April 28-May 2, 2013Albuquerque, NM, April 28-May 2, 2013. Available at http://pbadupws.nrc.gov/docs/ML1310/ML13108A030.pdf

ASTM. 2008. *Standard Guide for Drying Behavior of Spent Nuclear Fuel*. ASTM C 1553-08, ASTM International, West Conshohocken, Pennsylvania.

Arkhipov OP, AO Verkhovskaya, SA Kabakchi, and AN Ermakov. 2007. "Development and verification of a mathematical model of the radiolysis of water vapor." *Atomic Energy* 103(5):870.

Atkinson R, DL Baulch, RA Cox, JN Crowley, RF Hampson, RG Hynes, ME Jenkin, MJ Rossi, and J Troe. 2004. "Evaluated kinetic and photochemical data for atmospheric chemistry: Volume I – gas phase reactions of O_x, HO_x, NO_x and SO_x species." *Atmospheric Chemistry and Physics*, 4(6):1461-1738.

Bare WC and LD Torgerson. 2001. *Dry Cask Storage Characterization Project—Phase l: CASTOR V/21 Cask Opening And Examination*, NUREG/CR 6745, INEEL/EXT-01-00183, Rev. 1, Idaho National Engineering and Environmental Laboratory, Idaho Falls, Idaho.

Battino R and HL Clever. 1966. "The Solubility of Gases in Liquids." *Chemical Reviews,* 66(4):395-463.

Brown PN, and AC Hindmarsh. 1989. "Reduced storage matrix methods in stiff ODE systems." *Journal of Applied Mathematics and Computing*, 31(May 1989):40-91.

BSC – Bechtel SAIC Company. 2002. *Gamma and Neutron Radiolysis in the 21-PWR Waste Package from Ten to One Million Years.* 000-00C-DSU0-00700-00-00A Bechtel SAIC Company, Las Vegas, Nevada: Bechtel SAIC Company. ACC: MOL.20021004.0002.

BSC – Bechtel SAIC Company. 2004, *Technical Basis Document No. 7: In-Package Environment and Waste Form Degradation and Solubility*, Bechtel SAIC Company, LLC, Las Vegas, Nevada.

Bulearcă AM, I Călinescu, and V Lavric. 2010. "Model Studies of NOx and SOx Reactions in Flue Gas Treatment by Electron Beam," *U.P.B. Sci. Bull., Series B*, 72(1):101-112.

Dzantiev B.G, A.N. Ermakov, B.M. Zhitomirsky and V.N. PoPov. 1984. "Thermoradiation processes of energy-carrier production.*" Int. J. Hydrogen Energy*, 9(8): 723-728.

Engineering Tool Box. 2013. "Properties of Saturated Steam – SI Units, A Saturated Steam Table with steam properties as specific volume, density, specific enthalpy and specific entropy." Accessed September 10, 2013 at http://www.engineeringtoolbox.com/saturated-steam-properties-d_101.html

Hanson B, H Alsaed, C Stockman, D Enos, R Meyer, and K Sorenson. 2012a. *Gap Analysis to Support Extended Storage of Used Nuclear Fuel.* FCRD-USED-2011-000136 Rev. 0, PNNL-20509. Prepared for the U.S. Department of Energy Used Fuel Disposition Campaign, Washington, D.C.

Hanson B, H Alsaed, and C Stockman. 2012b. *Used Nuclear Fuel Storage and Transportation Data Gap Prioritization.* FCRD-USED-2012-000109 Draft, PNNL-21360. Prepared for the U.S. Department of Energy Used Fuel Disposition Campaign, Washington, D.C.

Hindmarsh AC. 1983. "ODEPACK, A Systematized Collection of ODE Solvers." In *Scientific Computing*, IMACS Transactions on Scientific Computation, Volume 1 edited by RS Stepleman, M Carver, R Peskin, WF Ames and WF Vichnevetsky, North-Holland, Amsterdam, pp 55-64.

McEachern, RJ, S Sunder, S P Taylor, DC Doern, NH Miller, and DD Wood. 1998. "The influence of nitrogen dioxide on the oxidation of UO_2 in air at temperatures below 275°C." *Journal of Nuclear Materials*, 255(2-3):234-242.

McKinnon, MA and AL Doherty. 1997. *Spent Nuclear Fuel Integrity During Dry Storage—Performance Tests and Demonstration*. PNNL-11576, Pacific Northwest National Laboratory, Richland, Washington.

Railsback, LB 2013. "The chemical composition of Earth's atmosphere IV: water vapor." Accessed September 10, 2013 at http://www.gly.uga.edu/railsback/Fundamentals/AtmosphereCompIV.pdf.

Suffield SR, JM Cuta, JA Fort, BA Collins, HE Adkins, and ER Siciliano. 2012.*Thermal Modeling of NUHOMS HSM-15 and HSM-1 Storage Modules at Calvert Cliffs Nuclear Power Station ISFSI*. PNNL-21788, Pacific Northwest National Laboratory, Richland, Washington.

Sunder P, and NH Miller. 1996. "Oxidation of CANDU uranium oxide fuel by air in gamma radiation at 150°C." *Journal of Nuclear Materials*, 231:121-131.

Wittman RS and EC Buck. 2012. "Sensitivity of UO_2 Stability in a Reducing Environment on Radiolysis Model Parameters." In *Actinides and Nuclear Energy Material, MRS Spring 2012 Proceedings*, vol. 1444, ed. D Andersson, et al. Cambridge University Press, Cambridge, United Kingdom. DOI:10.1557/opl.2012.1449.

APPENDIX A:
Reaction Rate Constants

rate-const.txt

No.	$k^{(0)}$	x	E_a	Reaction
1	6.02E+13	0	0.00E+00	N2+ + e- = N(4S) + N(2D)
2	2.41E+14	0	0.00E+00	e- + NO+ = N(2D) + O
3	6.02E+08	0	0.00E+00	e- + NO+ = NO
4	5.44E+11	0	0.00E+00	e- + NO2 + N2 = NO2- + N2
5	1.74E+11	0	0.00E+00	e- + O2 + N2 = O2- + N2
6	4.17E+15	-0.5	0.00E+00	CO2+ + e- = CO + O
7	3.77E+16	-0.5	0.00E+00	CO2+ + e- + N2 = CO2 + N2
8	3.39E+21	-2.5	0.00E+00	CO+ + e- + N2 = CO + N2
9	3.01E+11	0	0.00E+00	N2+ + NO = NO+ + N2
10	3.01E+11	0	0.00E+00	N2+ + O2 = O2+ + N2
11	5.00E+11	0	0.00E+00	N2+ + CO2 = N2 + CO2+
12	3.79E+11	0	0.00E+00	O2+ + NO = NO+ + O2
13	6.02E+13	0	0.00E+00	O2+ + NO2- = O2 + NO2
14	2.53E+14	0	0.00E+00	O2+ + O2- = O2 + O2
15	1.20E+15	0	0.00E+00	O2+ + O2- = O + O + O2
16	1.32E+10	0	0.00E+00	N(4S) + NO = N2 + O
17	3.55E+09	0	0.00E+00	N(4S) + NO2 = NO + NO
18	4.64E+09	0	0.00E+00	N(4S) + NO2 = N2O + O
19	1.08E+09	0	0.00E+00	N(4S) + NO2 = N2 + O2
20	1.39E+09	0	0.00E+00	N(4S) + NO2 = N2 + O + O
21	6.02E+04	0	0.00E+00	N(4S) + O2 = NO + O
22	2.23E+08	0	0.00E+00	N(4S) + O3 = NO + O2
23	1.81E+09	0	0.00E+00	N(4S) + N(4S) + N2 = N2 + N2
24	9.64E+08	0	0.00E+00	N(2D) + N2O = NO + N2
25	3.55E+10	0	0.00E+00	N(2D) + NO = N(4S) + NO
26	3.13E+09	0	0.00E+00	N(2D) + O2 = NO + O
27	7.83E+11	0	0.00E+00	N+ + CO2 = N + CO2+
28	2.89E+11	0	0.00E+00	N+ + NO2- = NO + NO
29	3.63E+10	0	0.00E+00	O + NO + N2 = NO2 + N2
30	6.02E+09	0	0.00E+00	O + NO2 = NO + O2
31	4.71E+10	0	0.00E+00	O + NO2 + N2 = NO3 + N2
32	2.03E+08	0	0.00E+00	O + O2 + N2 = O3 + N2
33	9.03E+09	0	2.24E+00	O + O3 = O2 + O2
34	5.80E+08	0	0.00E+00	O + O + N2 = O2 + N2
35	1.02E+10	0	0.00E+00	O + HNO2 = NO2 + OH
36	1.02E+10	0	0.00E+00	O + HNO3 = NO3 + OH
37	1.02E+10	0	0.00E+00	O + NO3 = NO2 + O2
38	2.68E+11	0	0.00E+00	OH + NO + N2 = HNO2 + N2
39	1.20E+12	0	0.00E+00	OH + NO2 + N2 = HNO3 + N2
40	3.61E+09	0	0.00E+00	OH + HNO2 = NO2 + H2O
41	9.03E+07	0	0.00E+00	OH + HNO3 = NO3 + H2O
42	7.83E+08	0	9.50E+02	OH + O3 = HO2 + O2
43	1.20E+10	0	0.00E+00	OH + NO3 = HO2 + NO2
44	9.03E+07	0	0.00E+00	CO + OH = CO2 + H
45	1.96E+10	0	0.00E+00	H + O2 + N2 = HO2 + N2
46	1.69E+10	0	0.00E+00	H + O3 = OH + O2
47	1.69E+11	0	4.40E+02	H + HO2 = OH + OH

48	2.55E+10	0	7.00E+02	H + HO2 = H2O + O
49	5.90E+07	0	0.00E+00	H2O+ + H2O = OH + H3O+
50	2.89E+09	0	0.00E+00	H3O+ + NO2- = H + NO2 + H2O
51	3.91E+12	-0.78	0.00E+00	CO2+ + O2 = O2+ + CO2
52	1.02E+12	0	0.00E+00	CO2+ + H2O = H2O+ + CO2
53	4.17E+15	-0.5	0.00E+00	CO2+ + O2- = CO2 + O2
54	6.02E+10	0	0.00E+00	CO+ + O2 = O2+ + CO
55	7.83E+10	0	0.00E+00	CO+ + H2O = H2O+ + CO
56	5.12E+11	0	0.00E+00	CO+ + CO2 = CO2+ + CO
57	3.76E+20	-2.5	0.00E+00	CO+ + O2- = CO2 + O
58	6.02E+11	0	0.00E+00	O+ + CO2 = O2+ + CO
59	1.81E+14	0	0.00E+00	NO2- + NO+ = NO2 + NO
60	2.41E+14	0	0.00E+00	O2- + NO+ = O2 + NO
61	4.82E+14	0	0.00E+00	O2- + NO2 = NO2- + O2
62	2.41E+08	0	0.00E+00	N + CO2 = NO + CO
63	5.30E+09	0	0.00E+00	HO2 + NO = NO2 + OH
64	2.23E+07	0	0.00E+00	HO2 + NO2 = HNO2 + O2
65	1.26E+09	0	0.00E+00	HO2 + NO3 = HNO3 + O2
66	1.81E+06	0	0.00E+00	HO2 + O3 = OH + O2 + O2
67	1.20E+11	0	0.00E+00	HO2 + OH = H2O + O2
68	9.64E+07	0	0.00E+00	NH3 + OH = H2O + NH2
69	2.86E+20	0	0.00E+00	NO + NH = N2 + OH
70	9.64E+09	0	0.00E+00	NH2 + NO = N2 + H2O
71	1.20E+10	0	0.00E+00	NH2 + NO2 = N2O + H2O
72	1.08E+07	0	0.00E+00	NO + O3 = NO2 + O2
73	1.57E+10	0	0.00E+00	NO + NO3 = NO2 + NO2
74	2.41E+05	0	0.00E+00	NO2 + NO3 = NO + NO2 + O2
75	1.31E+12	0	0.00E+00	NO2 + NO3 + N2 = N2O5 + N2
76	2.11E+04	0	0.00E+00	NO2 + O3 = NO3 + O2
77	5.40E+04	0	0.00E+00	NO2 + NO2 + H2O = HNO2 + HNO3
78	7.23E+01	0	0.00E+00	N2O5 + N2 = NO2 + NO3 + N2
79	1.02E-01	0	0.00E+00	NO + HNO3 = HNO2 + NO2
80	6.62E+03	0	0.00E+00	HNO2 + HNO3 = NO2 + NO2 + H2O
81	8.26E+10	-0.4	8.84E+00	HNO2 + HNO2 = NO + NO2 + H2O
82	1.51E-01	0	0.00E+00	N2O5 + H2O = HNO3 + HNO3
83	9.64E+09	0	3.25E+03	NO3 + CO = NO2 + CO2
84	6.32E+13	0	0.00E+00	NH3 + HNO2 = NH4NO2(s)
85	6.32E+13	0	0.00E+00	NH3 + HNO3 = NH4NO3(s)
86	1.00E+13	-1	0.00E+00	H + H + H2O = H2O + H2
87	1.40E+17	-2	0.00E+00	H + OH + H2O = H2O + H2O
88	6.00E+16	-2	0.00E+00	OH + OH + H2O = H2O2 + H2O
89	8.91E+09	0	2.50E+02	O + OH = O2 + H
90	1.56E+12	-0.8	0.00E+00	H + O2 + H2O = H2O + HO2
91	2.39E+10	0.09	7.10E+02	H + HO2 = H2 + O2
92	1.80E+09	0	0.00E+00	HO2 + HO2 = H2O2 + O2
93	4.71E+12	-1	0.00E+00	H + O + H2O = OH + H2O
94	1.02E+10	0	1.80E+03	H + H2O2 = H2O + OH
95	4.46E+09	0	4.77E+02	OH + H2O2 = H2O + HO2
96	2.53E+05	0.48	1.70E+03	OH + H2 = H2O + H
97	1.50E+06	1.14	5.00E+01	OH + OH = H2O + O
98	1.89E+07	0	9.00E+02	O + O + H2O = O2 + H2O
99	5.10E+01	2.67	3.16E+03	O + H2 = OH + H
100	2.51E+15	0	2.41E+04	H2O2 + H2O = OH + OH + H2O
101	1.00E+07	0	5.00E+03	H + H2O = H2 + OH
102	6.02E+13	0	0.00E+00	O+ + NO2- = O2 + NO
103	6.02E+08	0	0.00E+00	e- + O2+ = O2

104	6.02E+08	0	0.00E+00	e- + O+ = O
105	1.89E+07	0	9.00E+02	N + N + N2 = N2 + N2
106	6.02E+02	0	0.00E+00	e- + H3O+ = H2O + H
107	6.02E+02	0	0.00E+00	e- + H2O+ = H2O
108	6.02E+02	0	0.00E+00	e- + N+ = N
109	6.02E+02	0	0.00E+00	O2- + N+ = NO2
110	1.00E-09	0	0.00E+00	N(4S) = N
111	1.00E-09	0	0.00E+00	N(2D) = N

APPENDIX B: FORTRAN Listing

rad-gas-ppm-T.f (used for external air)

```
      IMPLICIT REAL*8 (a-h,o-z)
      INTEGER nstep,nvar,NMAX,KMAXX,coefs
      CHARACTER*256 CARD
      CHARACTER*8 sname
      character*15 name1,name2
      character*14 name3
      character*13 name4
      PARAMETER (NMAX=500,KMAXX=500)
      REAL*8 x1,x2,vstart(441),dvstart(441),vatoms(2,441),atoms(2,60)
      REAL*8 dv(NMAX),v(NMAX)
      REAL*8 Av,R,T0,rnws,G,rK,echrg,VA,VB,Dfcoefs
      DIMENSION rK(250),G(250),xbnd(20),Cbnd(63),G0(250),sname(250),
     1        vin(250),GN2(250),GO2(250),GN20(250),GO20(250),GCO2(250),
     1        GCO20(250),Ea(250),xpon(250),
     1        rK0(250)
      EXTERNAL f
      REAL*8 xp(KMAXX), yp(NMAX,KMAXX)
      DOUBLE PRECISION ATOL, RTOL, RWORK, T, TOUT, Y
      DIMENSION Y(3), ATOL(441), RWORK(5000000), IWORK(5000000),
     1              coefs(250,250,2),ncoef(250),Dfcoefs(63)
      COMMON /const/ Av,R,T0,rnws,G,GN2,GO2,GCO2,rK,echrg,VA,VB,
     1 coefs,ncoef,Dfcoefs,T,Rflow,Vcell,vin,xbnd,Cbnd,ton,toff,
     2 Ea,xpon,rK0,nreg


      nvar = 40               ! 40 species

C Initialization loop
      open(3,file="rad-gas.in",status="OLD")
        read(3,"(a256)") CARD
        read(CARD(15:256),*) doser,ton,toff,T       !  Gy/hr
        read(3,"(a256)") CARD
        read(CARD(15:256),*) nreg,(xbnd(n),n=1,nreg+1)
        read(3,"(a256)") CARD
        read(CARD(24:256),*) rvcell,rrflow
        read(3,"(1x)")
        do isp =1,nvar
          read(3,"(a256)") CARD
          read(CARD(15:256),*) (vstart(isp+nvar*(n-1)),n=1,nreg),
     1                Cbnd(isp),Dfcoefs(isp),g0(isp),
     1      gN20(isp),gO20(isp),gCO20(isp),atoms(1,isp),
     2      atoms(2,isp)
          read(CARD(1:14),"(i6,a8)") idum,sname(isp)
        enddo

      close(3)
```

```
      CALL getcon

      edot  = doser   ! rad/s
c      100.d0*(doser/3600.d0)   ! rad/s
      Rflow = rrflow/(60.d0*1000.d0)
      Vcell = rvcell/1000.d0

      do ir=1,nvar
         vin(ir) = vstart(ir+nvar)
         g(ir)   = g0(ir) * edot / (Av * echrg * 100.d0 * 100.d0)
         gN2(ir) = gN20(ir) * edot / (Av * echrg * 100.d0 * 100.d0)
         gO2(ir) = gO20(ir) * edot / (Av * echrg * 100.d0 * 100.d0)
         gCO2(ir) = gCO20(ir) * edot / (Av * echrg * 100.d0 * 100.d0)
      enddo

c      write(*,*) "Diffusion between regions on (1) or off (0)?"
      difon = 1
c      read(*,*) difon
      if (difon == 0) then
      do ir=1,nvar
        Dfcoefs(ir) = 0.d0
      enddo
      endif

c      nreg =  7               !  7 regions
      nvtot = nvar*nreg
      eps =  1.d-3
      h1 =   1.d-3
      hmin = 1.d-16
      kmax = KMAXX
      Nvals = 20000

      ITOL = 2
      RTOL = 1.1d-11
      ITASK = 1
      ISTATE = 1
      IOPT = 0
c        do ir=5,10
c          RWORK(ir)=0.d0
c          IWORK(ir)=0
c        enddo
c        IWORK(6)=10000
      LRW = 1000000
      LIW = 1000000
      JT = 2

      do 5 isp=1,nvtot
        ATOL(isp) = 1.1D-16
    5 continue

C  t = 0

      x2 = 0.d0

      name1="sys-H2O-r00.dat"
```

```
 name2="sys-CO3-r00.dat"
 name3="sys-Cl-r00.dat"
 name4="sys-U-r00.dat"


 do n=1,nreg
    if (n.lt.10) then
    write(name1(11:11),"(i1)") n
    write(name2(11:11),"(i1)") n
    write(name3(10:10),"(i1)") n
    write(name4(9:9),"(i1)") n
    else
    write(name1(10:11),"(i2)") n
    write(name2(10:11),"(i2)") n
    write(name3(9:10),"(i2)") n
    write(name4(8:9),"(i2)") n
    endif
    open(10+n,file=name1,status="UNKNOWN",recl=1024)
 enddo

 do n=1,nreg
   write(10+n,"('#  Time(s)',8x,42(a8,8x))")
1     (sname(isp),isp= 1,40)
 enddo

 do 500 iter=0,Nvals
 x1 =  x2
 x2 =  dexp((dlog(1.d0)-dlog(1.d-6))*dfloat(iter)
1           /dfloat(Nvals)+dlog(1.d-6))

 CALL DLSODA(f,nvtot,vstart,x1,x2,ITOL,RTOL,ATOL,ITASK,ISTATE,
1     IOPT,RWORK,LRW,IWORK,LIW,JDUM,JT)
 call f(nvtot,x2,vstart,dvstart)
 do ivar=1,nvtot
    dvstart(ivar) = dvstart(ivar)*Av*echrg*1.d7/
1                   (18.d0*doser*vstart(1))
 enddo

 do n=1,nreg

   testO = 0.d0
   testH = 0.d0
   totalM= 0.d0
   totalM= 0.d0
 do isp=1,40
   testO = testO + vstart(isp+nvar*(n-1))*atoms(2,isp)
   testH = testH + vstart(isp+nvar*(n-1))*atoms(1,isp)
   totalM= totalM+ vstart(isp+nvar*(n-1))
 enddo

   Tkelv = (T+T0 - 310.15d0)*decay(x2) + 310.15d0
   DdotT = decay2(x2)*edot*3600.
   write(10+n,"(45(1pe16.8))") x2/(365.25*24.*3600.),
1           ((vstart(isp+nvar*(n-1))*1.d6/totalM),isp= 1,40)
```

```
    2           ,(testH*1.d6)
    3           ,(testO*1.d6),Tkelv,DdotT
     enddo


  500 continue

     Nvals = 20000
     do 600 iter=1,Nvals
     x1 =  x2
     x2 =  dexp((dlog(1.d4)-dlog(1.d0))*dfloat(iter)
    1           /dfloat(Nvals)+dlog(1.d0))
     CALL DLSODA(f,nvtot,vstart,x1,x2,ITOL,RTOL,ATOL,ITASK,ISTATE,
    1     IOPT,RWORK,LRW,IWORK,LIW,JDUM,JT)
     call f(nvtot,x2,vstart,dvstart)
     do ivar=1,nvtot
        dvstart(ivar) = dvstart(ivar)*Av*echrg*1.d7/
    1                   (18.d0*doser*vstart(1))
     enddo

     do n=1,nreg

       testO = 0.d0
       testH = 0.d0
       totalM= 0.d0
     do isp=1,40
       testO = testO + vstart(isp+nvar*(n-1))*atoms(2,isp)
       testH = testH + vstart(isp+nvar*(n-1))*atoms(1,isp)
       totalM= totalM+ vstart(isp+nvar*(n-1))
     enddo
       Tkelv = (T+T0 - 310.15d0)*decay(x2) + 310.15d0
       DdotT = decay2(x2)*edot*3600.
       write(10+n,"(45(1pe16.8))") x2/(365.25*24.*3600.),
    1           ((vstart(isp+nvar*(n-1))*1.d6/totalM),isp= 1,40)
    2           ,(testH*1.d6)
    3           ,(testO*1.d6),Tkelv,DdotT
     enddo

  600 continue

     Nvals = 2000
     do 700 iter=1,Nvals
     x1 =  x2
     x2 =  dexp((dlog(1.d5)-dlog(1.d4))*dfloat(iter)
    1           /dfloat(Nvals)+dlog(1.d4))
     CALL DLSODA(f,nvtot,vstart,x1,x2,ITOL,RTOL,ATOL,ITASK,ISTATE,
    1     IOPT,RWORK,LRW,IWORK,LIW,JDUM,JT)
     call f(nvtot,x2,vstart,dvstart)
     do ivar=1,nvtot
        dvstart(ivar) = dvstart(ivar)*Av*echrg*1.d7/
    1                   (18.d0*doser*vstart(1))
     enddo
     do n=1,nreg

       testO = 0.d0
       testH = 0.d0
```

```
        totalM= 0.d0
      do isp=1,40
        testO = testO + vstart(isp+nvar*(n-1))*atoms(2,isp)
        testH = testH + vstart(isp+nvar*(n-1))*atoms(1,isp)
        totalM= totalM+ vstart(isp+nvar*(n-1))
      enddo
        Tkelv = (T+T0 - 310.15d0)*decay(x2) + 310.15d0
        DdotT = decay2(x2)*edot*3600.
        write(10+n,"(45(1pe16.8))") x2/(365.25*24.*3600.),
     1           ((vstart(isp+nvar*(n-1))*1.d6/totalM),isp= 1,40)
     2           ,(testH*1.d6)
     3           ,(testO*1.d6),Tkelv,DdotT
      enddo

  700 continue

c      goto 800
      Nvals = 20000
      do 800 iter=1,Nvals
      x1 =  x2
      x2 =  dexp((dlog(4.d5)-dlog(1.d5))*dfloat(iter)
     1           /dfloat(Nvals)+dlog(1.d5))
      CALL DLSODA(f,nvtot,vstart,x1,x2,ITOL,RTOL,ATOL,ITASK,ISTATE,
     1     IOPT,RWORK,LRW,IWORK,LIW,JDUM,JT)
      call f(nvtot,x2,vstart,dvstart)
      do ivar=1,nvtot
         dvstart(ivar) = dvstart(ivar)*Av*echrg*1.d7/
     1                   (18.d0*doser*vstart(1))
      enddo

      do n=1,nreg

        testO = 0.d0
        testH = 0.d0
        totalM= 0.d0
      do isp=1,40
        testO = testO + vstart(isp+nvar*(n-1))*atoms(2,isp)
        testH = testH + vstart(isp+nvar*(n-1))*atoms(1,isp)
        totalM= totalM+ vstart(isp+nvar*(n-1))
      enddo
        Tkelv = (T+T0 - 310.15d0)*decay(x2) + 310.15d0
        DdotT = decay2(x2)*edot*3600.
        write(10+n,"(45(1pe16.8))") x2/(365.25*24.*3600.),
     1           ((vstart(isp+nvar*(n-1))*1.d6/totalM),isp= 1,40)
     2           ,(testH*1.d6)
     3           ,(testO*1.d6),Tkelv,DdotT
      enddo

  800 continue

c      goto 900
      Nvals = 4000
      do 900 iter=1,Nvals
      x1 =  x2
```

```
      x2 =  dexp((dlog(1.d6)-dlog(4.d5))*dfloat(iter)
     1           /dfloat(Nvals)+dlog(4.d5))
      CALL DLSODA(f,nvtot,vstart,x1,x2,ITOL,RTOL,ATOL,ITASK,ISTATE,
     1     IOPT,RWORK,LRW,IWORK,LIW,JDUM,JT)
      call f(nvtot,x2,vstart,dvstart)
      do ivar=1,nvtot
         dvstart(ivar) = dvstart(ivar)*Av*echrg*1.d7/
     1                   (18.d0*doser*vstart(1))
      enddo

      do n=1,nreg

        testO = 0.d0
        testH = 0.d0
        totalM= 0.d0
      do isp=1,40
        testO = testO + vstart(isp+nvar*(n-1))*atoms(2,isp)
        testH = testH + vstart(isp+nvar*(n-1))*atoms(1,isp)
        totalM= totalM+ vstart(isp+nvar*(n-1))
      enddo
        Tkelv = (T+T0 - 310.15d0)*decay(x2) + 310.15d0
        DdotT = decay2(x2)*edot*3600.
        write(10+n,"(45(1pe16.8))") x2/(365.25*24.*3600.),
     1           ((vstart(isp+nvar*(n-1))*1.d6/totalM),isp= 1,40)
     2           ,(testH*1.d6)
     3           ,(testO*1.d6),Tkelv,DdotT
      enddo

  900 continue

c      goto 950
      Nvals = 40000
      do 950 iter=1,Nvals
      x1 =  x2
      x2 =  dexp((dlog(1.d10)-dlog(1.d6))*dfloat(iter)
     1           /dfloat(Nvals)+dlog(1.d6))
      CALL DLSODA(f,nvtot,vstart,x1,x2,ITOL,RTOL,ATOL,ITASK,ISTATE,
     1     IOPT,RWORK,LRW,IWORK,LIW,JDUM,JT)
      call f(nvtot,x2,vstart,dvstart)
      do ivar=1,nvtot
         dvstart(ivar) = dvstart(ivar)*Av*echrg*1.d7/
     1                   (18.d0*doser*vstart(1))
      enddo

      do n=1,nreg

        testO = 0.d0
        testH = 0.d0
        totalM= 0.d0
      do isp=1,40
        testO = testO + vstart(isp+nvar*(n-1))*atoms(2,isp)
        testH = testH + vstart(isp+nvar*(n-1))*atoms(1,isp)
        totalM= totalM+ vstart(isp+nvar*(n-1))
      enddo
        Tkelv = (T+T0 - 310.15d0)*decay(x2) + 310.15d0
        DdotT = decay2(x2)*edot*3600.
```

```
      write(10+n,"(45(1pe16.8))") x2/(365.25*24.*3600.),
    1           ((vstart(isp+nvar*(n-1))*1.d6/totalM),isp= 1,40)
    2           ,(testH*1.d6)
    3           ,(testO*1.d6),Tkelv,DdotT
     enddo

  950 continue

     do n=1,nreg
        close(10+n)
     enddo

     do 980 isp=1,nvtot
       if (vstart(isp).lt.1d-23) vstart(isp) = 0.d0
  980 continue

     open(3,file="rad-gas.in",status="OLD")
     open(4,file="rad-gas.out",status="UNKNOWN")
       read(3,"(a256)") CARD
       write(CARD(50:76),"('Final Time(s) = ',1pe11.3)") x2
       write(4,"(a256)") CARD
       read(3,"(a256)") CARD
       write(4,"(a256)") CARD
       read(3,"(a256)") CARD
       write(4,"(a256)") CARD
       read(3,"(a256)") CARD
       write(4,"(a)") CARD
       do isp =1,nvar
         read(3,"(a256)") CARD
         write(CARD(15:256),"(20(1pe11.3))")
    1               (vstart(isp+nvar*(n-1)),n=1,nreg),
    1   Cbnd(isp),Dfcoefs(isp),g0(isp),gN20(isp),gO20(isp),gCO20(isp)
    2           ,atoms(1,isp)
    3           ,atoms(2,isp)
         write(4,"(a)") CARD
       enddo

     close(3)
     close(4)

     stop
     END

     SUBROUTINE f(NEQ,x,u,du)
     IMPLICIT REAL*8 (a-h,o-z)
     INTEGER NMAX,coefs, nreg, nvar
     PARAMETER (NMAX=500)        !  Maximum number of functions
     REAL*8 x, du(*),u(*)
     REAL*8 Av,R,T0,rnws,G0, dum,
    1   rK,echrg,VA,VB,v,dv,Dfcoefs
     CHARACTER*256 CARD
     DIMENSION rK(250),G(250),RZ(250, 20), v(250, 20), dv(250, 20),
    1       coefs(250,250,2),ncoef(250),Dfcoefs(63),xbnd(20),Cbnd(63),
    1       vin(250),GN2(250),GO2(250),GCO2(250),Ea(250),xpon(250),
```

```
     1       rK0(250)
      COMMON /const/ Av,R,T0,rnws,G,GN2,GO2,GCO2,rK,echrg,VA,VB,
     1 coefs,ncoef,Dfcoefs,T,Rflow,Vcell,vin,xbnd,Cbnd,ton,toff,
     2 Ea,xpon,rK0,nreg

      dum=1

C  Species indexing: see kinetics.dat

      H2Oact = 55.56d0
      nvar = 40

C  u, du (1D) => v, dv (2D)
      do n=1, nreg
        do nspc = 1, nvar
           v(nspc,n) = u(nspc+nvar*(n-1))
           dv(nspc,n) = du(nspc+nvar*(n-1))
        enddo
      enddo

c      do icmp=1,nvar
c        vin(icmp) = 0.d0
c      enddo
      Tkelv = (T+T0 - 310.15d0)*decay(x) + 310.15d0
      do ir=1,111
                   rk(ir) =  rk0(ir)*
     1   dexp(-Ea(ir)/(Tkelv))*(Tkelv)**xpon(ir)
      enddo


C  Electrodynamic Terms
      do n=1, nreg
      RZ(  1,n) = rk(  1) * (v(15,n)**1) * (v(33,n)**1)
      RZ(  2,n) = rk(  2) * (v(15,n)**1) * (v(34,n)**1)
      RZ(  3,n) = rk(  3) * (v(15,n)**1) * (v(34,n)**1)
      RZ(  4,n) = rk(  4) * (v(15,n)**1) * (v(16,n)**1) * (v(21,n)**1)
      RZ(  5,n) = rk(  5) * (v( 7,n)**1) * (v(15,n)**1) * (v(16,n)**1)
      RZ(  6,n) = rk(  6) * (v(15,n)**1) * (v(39,n)**1)
      RZ(  7,n) = rk(  7) * (v(15,n)**1) * (v(16,n)**1) * (v(39,n)**1)
      RZ(  8,n) = rk(  8) * (v(15,n)**1) * (v(16,n)**1) * (v(38,n)**1)
      RZ(  9,n) = rk(  9) * (v(20,n)**1) * (v(33,n)**1)
      RZ( 10,n) = rk( 10) * (v( 7,n)**1) * (v(33,n)**1)
      RZ( 11,n) = rk( 11) * (v(33,n)**1) * (v(36,n)**1)
      RZ( 12,n) = rk( 12) * (v(11,n)**1) * (v(20,n)**1)
      RZ( 13,n) = rk( 13) * (v(11,n)**1) * (v(32,n)**1)
      RZ( 14,n) = rk( 14) * (v(10,n)**1) * (v(11,n)**1)
      RZ( 15,n) = rk( 15) * (v(10,n)**1) * (v(11,n)**1)
      RZ( 16,n) = rk( 16) * (v(19,n)**1) * (v(20,n)**1)
      RZ( 17,n) = rk( 17) * (v(19,n)**1) * (v(21,n)**1)
      RZ( 18,n) = rk( 18) * (v(19,n)**1) * (v(21,n)**1)
      RZ( 19,n) = rk( 19) * (v(19,n)**1) * (v(21,n)**1)
      RZ( 20,n) = rk( 20) * (v(19,n)**1) * (v(21,n)**1)
      RZ( 21,n) = rk( 21) * (v( 7,n)**1) * (v(19,n)**1)
      RZ( 22,n) = rk( 22) * (v( 9,n)**1) * (v(19,n)**1)
      RZ( 23,n) = rk( 23) * (v(16,n)**1) * (v(19,n)**2)
      RZ( 24,n) = rk( 24) * (v(18,n)**1) * (v(23,n)**1)
```

```
RZ( 25,n) = rk( 25) * (v(18,n)**1) * (v(20,n)**1)
RZ( 26,n) = rk( 26) * (v( 7,n)**1) * (v(18,n)**1)
RZ( 27,n) = rk( 27) * (v(35,n)**1) * (v(36,n)**1)
RZ( 28,n) = rk( 28) * (v(32,n)**1) * (v(35,n)**1)
RZ( 29,n) = rk( 29) * (v( 8,n)**1) * (v(16,n)**1) * (v(20,n)**1)
RZ( 30,n) = rk( 30) * (v( 8,n)**1) * (v(21,n)**1)
RZ( 31,n) = rk( 31) * (v( 8,n)**1) * (v(16,n)**1) * (v(21,n)**1)
RZ( 32,n) = rk( 32) * (v( 7,n)**1) * (v( 8,n)**1) * (v(16,n)**1)
RZ( 33,n) = rk( 33) * (v( 8,n)**1) * (v( 9,n)**1)
RZ( 34,n) = rk( 34) * (v( 8,n)**2) * (v(16,n)**1)
RZ( 35,n) = rk( 35) * (v( 8,n)**1) * (v(24,n)**1)
RZ( 36,n) = rk( 36) * (v( 8,n)**1) * (v(25,n)**1)
RZ( 37,n) = rk( 37) * (v( 8,n)**1) * (v(22,n)**1)
RZ( 38,n) = rk( 38) * (v( 4,n)**1) * (v(16,n)**1) * (v(20,n)**1)
RZ( 39,n) = rk( 39) * (v( 4,n)**1) * (v(16,n)**1) * (v(21,n)**1)
RZ( 40,n) = rk( 40) * (v( 4,n)**1) * (v(24,n)**1)
RZ( 41,n) = rk( 41) * (v( 4,n)**1) * (v(25,n)**1)
RZ( 42,n) = rk( 42) * (v( 4,n)**1) * (v( 9,n)**1)
RZ( 43,n) = rk( 43) * (v( 4,n)**1) * (v(22,n)**1)
RZ( 44,n) = rk( 44) * (v( 4,n)**1) * (v(37,n)**1)
RZ( 45,n) = rk( 45) * (v( 3,n)**1) * (v( 7,n)**1) * (v(16,n)**1)
RZ( 46,n) = rk( 46) * (v( 3,n)**1) * (v( 9,n)**1)
RZ( 47,n) = rk( 47) * (v( 3,n)**1) * (v( 5,n)**1)
RZ( 48,n) = rk( 48) * (v( 3,n)**1) * (v( 5,n)**1)
RZ( 49,n) = rk( 49) * (v( 1,n)**1) * (v(13,n)**1)
RZ( 50,n) = rk( 50) * (v(14,n)**1) * (v(32,n)**1)
RZ( 51,n) = rk( 51) * (v( 7,n)**1) * (v(39,n)**1)
RZ( 52,n) = rk( 52) * (v( 1,n)**1) * (v(39,n)**1)
RZ( 53,n) = rk( 53) * (v(10,n)**1) * (v(39,n)**1)
RZ( 54,n) = rk( 54) * (v( 7,n)**1) * (v(38,n)**1)
RZ( 55,n) = rk( 55) * (v( 1,n)**1) * (v(38,n)**1)
RZ( 56,n) = rk( 56) * (v(36,n)**1) * (v(38,n)**1)
RZ( 57,n) = rk( 57) * (v(10,n)**1) * (v(38,n)**1)
RZ( 58,n) = rk( 58) * (v(12,n)**1) * (v(36,n)**1)
RZ( 59,n) = rk( 59) * (v(32,n)**1) * (v(34,n)**1)
RZ( 60,n) = rk( 60) * (v(10,n)**1) * (v(34,n)**1)
RZ( 61,n) = rk( 61) * (v(10,n)**1) * (v(21,n)**1)
RZ( 62,n) = rk( 62) * (v(17,n)**1) * (v(36,n)**1)
RZ( 63,n) = rk( 63) * (v( 5,n)**1) * (v(20,n)**1)
RZ( 64,n) = rk( 64) * (v( 5,n)**1) * (v(21,n)**1)
RZ( 65,n) = rk( 65) * (v( 5,n)**1) * (v(22,n)**1)
RZ( 66,n) = rk( 66) * (v( 5,n)**1) * (v( 9,n)**1)
RZ( 67,n) = rk( 67) * (v( 4,n)**1) * (v( 5,n)**1)
RZ( 68,n) = rk( 68) * (v( 4,n)**1) * (v(28,n)**1)
RZ( 69,n) = rk( 69) * (v(20,n)**1) * (v(26,n)**1)
RZ( 70,n) = rk( 70) * (v(20,n)**1) * (v(27,n)**1)
RZ( 71,n) = rk( 71) * (v(21,n)**1) * (v(27,n)**1)
RZ( 72,n) = rk( 72) * (v( 9,n)**1) * (v(20,n)**1)
RZ( 73,n) = rk( 73) * (v(20,n)**1) * (v(22,n)**1)
RZ( 74,n) = rk( 74) * (v(21,n)**1) * (v(22,n)**1)
RZ( 75,n) = rk( 75) * (v(16,n)**1) * (v(21,n)**1) * (v(22,n)**1)
RZ( 76,n) = rk( 76) * (v( 9,n)**1) * (v(21,n)**1)
RZ( 77,n) = rk( 77) * (v( 1,n)**1) * (v(21,n)**2)
RZ( 78,n) = rk( 78) * (v(16,n)**1) * (v(29,n)**1)
```

```
      RZ( 79,n) = rk( 79) * (v(20,n)**1) * (v(25,n)**1)
      RZ( 80,n) = rk( 80) * (v(24,n)**1) * (v(25,n)**1)
      RZ( 81,n) = rk( 81) * (v(24,n)**2)
      RZ( 82,n) = rk( 82) * (v( 1,n)**1) * (v(29,n)**1)
      RZ( 83,n) = rk( 83) * (v(22,n)**1) * (v(37,n)**1)
      RZ( 84,n) = rk( 84) * (v(24,n)**1) * (v(28,n)**1)
      RZ( 85,n) = rk( 85) * (v(25,n)**1) * (v(28,n)**1)
      RZ( 86,n) = rk( 86) * (v( 1,n)**1) * (v( 3,n)**2)
      RZ( 87,n) = rk( 87) * (v( 1,n)**1) * (v( 3,n)**1) * (v( 4,n)**1)
      RZ( 88,n) = rk( 88) * (v( 1,n)**1) * (v( 4,n)**2)
      RZ( 89,n) = rk( 89) * (v( 4,n)**1) * (v( 8,n)**1)
      RZ( 90,n) = rk( 90) * (v( 1,n)**1) * (v( 3,n)**1) * (v( 7,n)**1)
      RZ( 91,n) = rk( 91) * (v( 3,n)**1) * (v( 5,n)**1)
      RZ( 92,n) = rk( 92) * (v( 5,n)**2)
      RZ( 93,n) = rk( 93) * (v( 1,n)**1) * (v( 3,n)**1) * (v( 8,n)**1)
      RZ( 94,n) = rk( 94) * (v( 2,n)**1) * (v( 3,n)**1)
      RZ( 95,n) = rk( 95) * (v( 2,n)**1) * (v( 4,n)**1)
      RZ( 96,n) = rk( 96) * (v( 4,n)**1) * (v( 6,n)**1)
      RZ( 97,n) = rk( 97) * (v( 4,n)**2)
      RZ( 98,n) = rk( 98) * (v( 1,n)**1) * (v( 8,n)**2)
      RZ( 99,n) = rk( 99) * (v( 6,n)**1) * (v( 8,n)**1)
      RZ(100,n) = rk(100) * (v( 1,n)**1) * (v( 2,n)**1)
      RZ(101,n) = rk(101) * (v( 1,n)**1) * (v( 3,n)**1)
      RZ(102,n) = rk(102) * (v(12,n)**1) * (v(32,n)**1)
      RZ(103,n) = rk(103) * (v(11,n)**1) * (v(15,n)**1)
      RZ(104,n) = rk(104) * (v(12,n)**1) * (v(15,n)**1)
      RZ(105,n) = rk(105) * (v(16,n)**1) * (v(17,n)**2)
      RZ(106,n) = rk(106) * (v(14,n)**1) * (v(15,n)**1)
      RZ(107,n) = rk(107) * (v(13,n)**1) * (v(15,n)**1)
      RZ(108,n) = rk(108) * (v(15,n)**1) * (v(35,n)**1)
      RZ(109,n) = rk(109) * (v(10,n)**1) * (v(35,n)**1)
      RZ(110,n) = rk(110) * (v(19,n)**1)
      RZ(111,n) = rk(111) * (v(18,n)**1)
      enddo

C  Reactions



      do n=1,nreg

        do icmp=1,nvar

          dv( icmp,n) = 0.d0
c          if(n.eq.1)
c           if((x.ge.ton).and.(x.le.toff))
          dv( icmp,n) =
     1      ( g( icmp)  * (v( 1,n)/H2Oact) +
     2        gN2( icmp)* (v(16,n)*28.d0/(H2Oact*18.d0)) +
     2        gCO2(icmp)* (v(36,n)*44.d0/(H2Oact*18.d0)) +
     3        gO2( icmp)* (v( 7,n)*32.d0/(H2Oact*18.d0)) )*decay2(x)
     4         *(sign(1.d0,x - ton) - sign(1.d0,x - toff))/2.d0
          if(icmp.ne.1000) then
          do icoef=1,ncoef(icmp)
            dv(icmp,n) = dv(icmp,n) + dfloat(coefs(icmp,icoef,2))
     1                                *RZ(coefs(icmp,icoef,1),n)
```

```
      enddo
      elseif(n.ne.1) then
      do icoef=1,ncoef(icmp)
        dv(icmp,n) = dv(icmp,n) + dfloat(coefs(icmp,icoef,2))
1                                 *RZ(coefs(icmp,icoef,1),n-1)
      enddo
      endif

       time = 0.d0
       dnorm = (1408.21d0*dexp(-0.0244196d0*time) +
1               6742.45d0*dexp(-0.322624d0*time)) /
1         (1408.21d0 + 6742.45d0)

      dv( icmp,n) = dv( icmp,n)
1             + (vin(icmp) - v( icmp,n))*(Rflow/Vcell)
2    *(decay2(x)*0.99d0 +0.01d0)/dnorm

    enddo

  enddo


  do icmp=1,nvar

  n=1
           xp12 = (xbnd(n)   + xbnd(n+1))/2.d0
           xp32 = (xbnd(n+1) + xbnd(n+2))/2.d0
    dv(icmp,n) = dv(icmp,n) +
1    (  (
3  v(icmp,n)  /(xp12-xp32)
4+ v(icmp,n+1)/(xp32-xp12)
5                             )   )
1          *Dfcoefs(icmp)/(xbnd(n+1)-xbnd(n))

  do n=2,nreg-1
           xm12 = (xbnd(n-1) + xbnd(n)  )/2.d0
           xp12 = (xbnd(n)   + xbnd(n+1))/2.d0
           xp32 = (xbnd(n+1) + xbnd(n+2))/2.d0
    dv(icmp,n) = dv(icmp,n) +
1    (   (
3  v(icmp,n)  /(xp12-xp32)
4+ v(icmp,n+1)/(xp32-xp12)
5                             ) + (
6  v(icmp,n-1)/(xp12-xm12)
7+ v(icmp,n)  /(xm12-xp12)
9                                                        )   )
1          *Dfcoefs(icmp)/(xbnd(n+1)-xbnd(n))
  enddo

  n = nreg

  if (Cbnd(icmp).ge.-0.5d0) then
           xm12 = (xbnd(n-1) + xbnd(n)  )/2.d0
           xp12 = (xbnd(n)   + xbnd(n+1))/2.d0
```

```
              xp32 = (xbnd(n+1) + xbnd(n+1))/2.d0
        dv(icmp,n) = dv(icmp,n) +
     1    (   (
     3  v(icmp,n)  /(xp12-xp32)
     4+   Cbnd(icmp)/(xp32-xp12)
     5                              ) + (
     6  v(icmp,n-1)/(xp12-xm12)
     7+ v(icmp,n)  /(xm12-xp12)
     9                                                    )   )
     1          *Dfcoefs(icmp)/(xbnd(n+1)-xbnd(n))
      else
              xm12 = (xbnd(n-1) + xbnd(n)  )/2.d0
              xp12 = (xbnd(n)   + xbnd(n+1))/2.d0
        dv(icmp,n) = dv(icmp,n) +
     1    (   (
     6  v(icmp,n-1)/(xp12-xm12)
     7+ v(icmp,n)  /(xm12-xp12)
     5                              )    )
     1          *Dfcoefs(icmp)/(xbnd(n+1)-xbnd(n))
      endif

      enddo


C  v, dv (2D) => u, du (1D)
      do n=1, nreg
        do nspc = 1, nvar
           u(nspc+nvar*(n-1)) = v(nspc,n)
           du(nspc+nvar*(n-1)) = dv(nspc,n)
        enddo
      enddo

      return
      END

      SUBROUTINE getcon
      IMPLICIT REAL*8 (a-h,o-z)
      INTEGER NMAX,coefs
      PARAMETER (NMAX=250)
      REAL*8 Av,R,T0,rnws,G0,RKeq,
     1   rK,VA,VB,Dfcoefs,Cbnd(63)
      CHARACTER*512 CARD
      DIMENSION rK(250),g(250),RKeq(10),xbnd(20),
     1  coefs(250,250,2),ncoef(250),Dfcoefs(63),
     2  vin(250),GN2(250),GO2(250),GCO2(250),Ea(250),xpon(250),rK0(250)
      COMMON /const/ Av,R,T0,rnws,G,GN2,GO2,GCO2,rK,echrg,VA,VB,
     1 coefs,ncoef,Dfcoefs,T,Rflow,Vcell,vin,xbnd,Cbnd,ton,toff,
     2 Ea,xpon,rK0,nreg

      nvar = 40

C   Physical constants
      Av    =   6.0221415d23 !  mole^{-1}
      R     =   8.31447d0    !  J mole^{-1} K^{-1}
      echrg =   1.602176462d-19 !  J/eV
      T0    = 273.15d0       !  K @ 0 C
```

```
      rnws  = 2.d-3   !  moles/cm^3,  Density of
                      !  saturated water vapor at 288 C
      VA    = 0.2d0   ! cm^3
      VB    = 23.d0   ! cm^3

c      edot  = radon *   25.d0  ! rad/s

      do ir=1,10
         RKeq(ir) = 0.d0
      enddo

      do ir=1,250
         rk(ir) = 0.d0
      enddo


C
C  Equilibrium and rate constants from:
C    Barbara Pastina and Jay A. LaVerne, J. Phys. Chem. A 2001, 105, 9316-93.
C
C    Equilibria  10^(-pKa)
      RKeq(2) = 10.d0**(-13.999d0)   !  H2O  <--> H+  +  OH-
      RKeq(3) = 10.d0**(-11.65d0)    !  H2O2 <--> H+  +  HO2-
      RKeq(4) = 10.d0**(-11.9d0)     !  OH   <--> H+  +  O-
      RKeq(5) = 10.d0**(- 4.57d0)    !  HO2  <--> H+  +  O2-
      RKeq(6) = 10.d0**(- 9.77d0)    !  H    <--> H+  +  e-
C    Rate coefficients  (M-1 s-1 or s-1)

      H2O = 1.d0       ! For now water is a dummy species
      H2Oact = 55.56d0  ! For now water is a dummy species

      open(3,file='rate-const.txt',status='OLD')
      do ir=1,111
         read(3,*) ireac,rk0(ireac),xpon(ireac),Ea(ireac)
                   rk(ireac) =  rk0(ireac)*
     1        dexp(-Ea(ireac)/(T+T0))*(T+T0)**xpon(ireac)
      enddo
      close(3)

c      rk( 2)   =  rk( 1)*RKeq(2)
c      rk( 3)   =  rk( 4)*RKeq(3)
c      rk( 6)   =  rk( 5)*RKeq(2)/ RKeq(3)
c      rk( 9)   =  rk(10)*RKeq(6)
c      rk(12)   =  rk(11)*RKeq(2)/ RKeq(4)
c      rk(13)   =  rk(14)*RKeq(4)
c      rk(15)   =  rk(16)*RKeq(5)
c      rk(18)   =  rk(17)*RKeq(2)/ RKeq(5)

      open(3,file='kinetics.dat',status='OLD')
      do ic=1,40
        read(3,"(a)") CARD
        read(CARD(1:10),*)    icomp,  ncoef(icomp)
        read(CARD(20:512),*) (coefs(icomp,icoef,1),icoef=1,ncoef(icomp))
        read(3,"(a)") CARD
```

```
        read(CARD(20:512),*) (coefs(icomp,icoef,2),icoef=1,ncoef(icomp))
      enddo
      close(3)

      return
      END

      function decay(x)
      real*8 x,t,decay
c   Fit to decay curve
   a0 = 1408.21
   a1 = 0.0244196
   a2 = 6742.45
   a3 = 0.322624

            t = 0.d0 + x/(365.25d0*24.d0*3600.d0)
            decay = dexp(-0.0231049d0*t)

      decay = 1.d0

      RETURN
      end

      function decay2(x)
      real*8 x,t,decay2
c   Fit to decay curve
   a0 = 1408.21
   a1 = 0.0244196
   a2 = 6742.45
   a3 = 0.322624

            t = 0.d0+x/(365.25d0*24.d0*3600.d0)
            decay2 = (1408.21d0*dexp(-0.0244196d0*t) +
     1              6742.45d0*dexp(-0.322624d0*t)) /
     1        (1408.21d0 + 6742.45d0)

c      decay2 = 1.d0

      RETURN
      end
```

APPENDIX C: Initial Gas Composition

rad-gas.in (100% RH air at 37C):

```
Dose [rad/s]          2.264     -1.d0    1.e11      37.
RegBndys (cm)     2    0.d0  3.d-3 3.d-2  3.d-1 3.d0   3.d1
Flow Vol(cc),R(cc/min)       1440.d0    1.0d0                                [G/100 eV]
0     Species   [reg1]    [reg2]        [Bndy]  [Dcm^2/s]      H2O          N2           O2           CO2
1     H2O       2.422d-03 2.422d-03 -1.000d+00 1.000d+00 -7.350d+00  0.000d+00  0.000d+00  0.000d+00  2.  1
2     H2O2      0.000d-01 0.000d-01 -1.000d+00 1.000d+00  0.000d+00  0.000d+00  0.000d+00  0.000d+00  2.  2
3     H         0.000d-01 0.000d-01 -1.000d+00 1.000d+00  7.400d+00  0.000d+00  0.000d+00  0.000d+00  1.  0
4     OH        0.000d-01 0.000d-01 -1.000d+00 1.000d+00  6.300d+00  0.000d+00  0.000d+00  0.000d+00  1.  1
5     HO2       0.000d-01 0.000d-01 -1.000d+00 1.000d+00  0.000d+00  0.000d+00  0.000d+00  0.000d+00  1.  2
6     H2        2.407E-08 2.407E-08 -1.000d+00 1.000d+00  0.500d+00  0.000d+00  0.000d+00  0.000d+00  2.  0
7     O2        8.369E-03 8.369E-03 -1.000d+00 1.000d+00  0.000d+00  0.000d+00 -5.300d+00  0.000d+00  0.  2
8     O         0.000d-01 0.000d-01 -1.000d+00 1.000d+00  1.050d+00  0.000d+00  5.230d+00  5.020d+00  0.  1
9     O3        1.532E-09 1.532E-09 -1.000d+00 1.000d+00  0.000d+00  0.000d+00  0.000d+00  0.000d+00  0.  3.
10    O2-       0.000d-01 0.000d-01 -1.000d+00 1.000d+00  0.000d+00  0.000d+00  0.000d+00  0.000d+00  0.  2.
11    O2+       0.000d-01 0.000d-01 -1.000d+00 1.000d+00  0.000d+00  0.000d+00  2.070d+00  0.000d+00  0.  2.
12    O+        0.000d-01 0.000d-01 -1.000d+00 1.000d+00  0.000d+00  0.000d+00  1.230d+00  0.210d+00  0.  1.
13    H2O+      0.000d-01 0.000d-01 -1.000d+00 1.000d+00  0.000d+00  0.000d+00  0.000d+00  0.000d+00  2.  1.
14    H3O+      0.000d-01 0.000d-01 -1.000d+00 1.000d+00  0.000d+00  0.000d+00  0.000d+00  0.000d+00  3.  1.
15    e-        0.000d-01 0.000d-01 -1.000d+00 1.000d+00  0.000d+00  2.960d+00  3.300d+00  2.960d+00  0.  0.
16    N2        3.120E-02 3.120E-02 -1.000d+00 1.000d+00  0.000d+00 -4.140d+00  0.000d+00  0.000d+00  0.  0.
17    N         0.000d-01 0.000d-01 -1.000d+00 1.000d+00  0.000d+00  0.295d+00  0.000d+00  0.000d+00  0.  0.
18    N(2D)     0.000d-01 0.000d-01 -1.000d+00 1.000d+00  0.000d+00  0.885d+00  0.000d+00  0.000d+00  0.  0.
19    N(4S)     0.000d-01 0.000d-01 -1.000d+00 1.000d+00  0.000d+00  1.870d+00  0.000d+00  0.000d+00  0.  0.
20    NO        0.000d-01 0.000d-01 -1.000d+00 1.000d+00  0.000d+00  0.000d+00  0.000d+00  0.000d+00  0.  1.
21    NO2       8.754E-10 8.754E-10 -1.000d+00 1.000d+00  0.000d+00  0.000d+00  0.000d+00  0.000d+00  0.  2.
22    NO3       0.000d-01 0.000d-01 -1.000d+00 1.000d+00  0.000d+00  0.000d+00  0.000d+00  0.000d+00  0.  3.
23    N2O       1.422E-08 1.422E-08 -1.000d+00 1.000d+00  0.000d+00  0.000d+00  0.000d+00  0.000d+00  0.  1.
24    HNO2      0.000d-01 0.000d-01 -1.000d+00 1.000d+00  0.000d+00  0.000d+00  0.000d+00  0.000d+00  1.  2.
25    HNO3      0.000d-01 0.000d-01 -1.000d+00 1.000d+00  0.000d+00  0.000d+00  0.000d+00  0.000d+00  1.  3.
26    NH        0.000d-01 0.000d-01 -1.000d+00 1.000d+00  0.000d+00  0.000d+00  0.000d+00  0.000d+00  1.  0.
27    NH2       0.000d-01 0.000d-01 -1.000d+00 1.000d+00  0.000d+00  0.000d+00  0.000d+00  0.000d+00  2.  0.
28    NH3       0.000d-01 0.000d-01 -1.000d+00 1.000d+00  0.000d+00  0.000d+00  0.000d+00  0.000d+00  3.  0.
29    N2O5      0.000d-01 0.000d-01 -1.000d+00 1.000d+00  0.000d+00  0.000d+00  0.000d+00  0.000d+00  0.  5.
30    NH4NO2    0.000d-01 0.000d-01 -1.000d+00 1.000d+00  0.000d+00  0.000d+00  0.000d+00  0.000d+00  4.  2.
31    NH4NO3    0.000d-01 0.000d-01 -1.000d+00 1.000d+00  0.000d+00  0.000d+00  0.000d+00  0.000d+00  4.  3.
32    NO2-      0.000d-01 0.000d-01 -1.000d+00 1.000d+00  0.000d+00  0.000d+00  0.000d+00  0.000d+00  0.  2.
33    N2+       0.000d-01 0.000d-01 -1.000d+00 1.000d+00  0.000d+00  2.270d+00  0.000d+00  0.000d+00  0.  0.
34    NO+       0.000d-01 0.000d-01 -1.000d+00 1.000d+00  0.000d+00  0.000d+00  0.000d+00  0.000d+00  0.  1.
35    N+        0.000d-01 0.000d-01 -1.000d+00 1.000d+00  0.000d+00  0.690d+00  0.000d+00  0.000d+00  0.  0.
36    CO2       1.590E-05 1.590E-05 -1.000d+00 1.000d+00  0.000d+00  0.000d+00  0.000d+00 -7.470d+00  0.  2.
37    CO        4.377E-09 4.377E-09 -1.000d+00 1.000d+00  0.000d+00  0.000d+00  0.000d+00  4.720d+00  0.  1.
38    CO+       0.000d-01 0.000d-01 -1.000d+00 1.000d+00  0.000d+00  0.000d+00  0.000d+00  0.510d+00  0.  1.
39    CO2+      0.000d-01 0.000d-01 -1.000d+00 1.000d+00  0.000d+00  0.000d+00  0.000d+00  2.240d+00  0.  2.
40    He        0.000d-01 0.000d-01 -1.000d+00 1.000d+00  0.000d+00  0.000d+00  0.000d+00  0.000d+00  0.  0.
```

rad-gas.in (He [5-atm] Fill Gas, 1-L water, 0.1% air):

```
Dose [rad/s]        53.38d0     -1.d0    1.e11      300.
RegBndys (cm)     2    0.d0  3.d-3 3.d-2  3.d-1 3.d0  3.d1
Flow Vol(cc),R(cc/min)        1440.d0    0.0d0                                    [G/100 eV]
0     Species    [reg1]    [reg2]        [Bndy]  [Dcm^2/s]      H2O         N2          O2          CO2
1     H2O       1.234d-02 1.234d-02 -1.000d+00 1.000d+00 -7.350d+00  0.000d+00  0.000d+00  0.000d+00  2.  1
2     H2O2      0.000d+00 0.000d+00 -1.000d+00 1.000d+00  0.000d+00  0.000d+00  0.000d+00  0.000d+00  2.  2
3     H         0.000d+00 0.000d+00 -1.000d+00 1.000d+00  7.400d+00  0.000d+00  0.000d+00  0.000d+00  1.  0
4     OH        0.000d+00 0.000d+00 -1.000d+00 1.000d+00  6.300d+00  0.000d+00  0.000d+00  0.000d+00  1.  1
5     HO2       0.000d+00 0.000d+00 -1.000d+00 1.000d+00  0.000d+00  0.000d+00  0.000d+00  0.000d+00  1.  2
6     H2        0.000d+00 0.000d+00 -1.000d+00 1.000d+00  0.500d+00  0.000d+00  0.000d+00  0.000d+00  2.  0
7     O2        4.290d-05 4.290d-05 -1.000d+00 1.000d+00  0.000d+00  0.000d+00 -5.300d+00  0.000d+00  0.  2
8     O         0.000d+00 0.000d+00 -1.000d+00 1.000d+00  1.050d+00  0.000d+00  5.230d+00  5.020d+00  0.  1
9     O3        0.000d+00 0.000d+00 -1.000d+00 1.000d+00  0.000d+00  0.000d+00  0.000d+00  0.000d+00  0.  3.
10    O2-       0.000d+00 0.000d+00 -1.000d+00 1.000d+00  0.000d+00  0.000d+00  0.000d+00  0.000d+00  0.  2.
11    O2+       0.000d+00 0.000d+00 -1.000d+00 1.000d+00  0.000d+00  0.000d+00  2.070d+00  0.000d+00  0.  2.
12    O+        0.000d+00 0.000d+00 -1.000d+00 1.000d+00  0.000d+00  0.000d+00  1.230d+00  0.210d+00  0.  1.
13    H2O+      0.000d+00 0.000d+00 -1.000d+00 1.000d+00  0.000d+00  0.000d+00  0.000d+00  0.000d+00  2.  1.
14    H3O+      0.000d+00 0.000d+00 -1.000d+00 1.000d+00  0.000d+00  0.000d+00  0.000d+00  0.000d+00  3.  1.
15    e-        0.000d+00 0.000d+00 -1.000d+00 1.000d+00  0.000d+00  2.960d+00  3.300d+00  2.960d+00  0.  0.
16    N2        1.593d-04 1.593d-04 -1.000d+00 1.000d+00  0.000d+00 -4.140d+00  0.000d+00  0.000d+00  0.  0.
17    N         0.000d+00 0.000d+00 -1.000d+00 1.000d+00  0.000d+00  0.295d+00  0.000d+00  0.000d+00  0.  0.
18    N(2D)     0.000d-01 0.000d-01 -1.000d+00 1.000d+00  0.000d+00  0.885d+00  0.000d+00  0.000d+00  0.  0.
19    N(4S)     0.000d-01 0.000d-01 -1.000d+00 1.000d+00  0.000d+00  1.870d+00  0.000d+00  0.000d+00  0.  0.
20    NO        0.000d-01 0.000d-01 -1.000d+00 1.000d+00  0.000d+00  0.000d+00  0.000d+00  0.000d+00  0.  1.
21    NO2       0.000d+00 0.000d+00 -1.000d+00 1.000d+00  0.000d+00  0.000d+00  0.000d+00  0.000d+00  0.  2.
22    NO3       0.000d+00 0.000d+00 -1.000d+00 1.000d+00  0.000d+00  0.000d+00  0.000d+00  0.000d+00  0.  3.
23    N2O       0.000d+00 0.000d+00 -1.000d+00 1.000d+00  0.000d+00  0.000d+00  0.000d+00  0.000d+00  0.  1.
24    HNO2      0.000d+00 0.000d+00 -1.000d+00 1.000d+00  0.000d+00  0.000d+00  0.000d+00  0.000d+00  1.  2.
25    HNO3      0.000d+00 0.000d+00 -1.000d+00 1.000d+00  0.000d+00  0.000d+00  0.000d+00  0.000d+00  1.  3.
26    NH        0.000d+00 0.000d+00 -1.000d+00 1.000d+00  0.000d+00  0.000d+00  0.000d+00  0.000d+00  1.  0.
27    NH2       0.000d+00 0.000d+00 -1.000d+00 1.000d+00  0.000d+00  0.000d+00  0.000d+00  0.000d+00  2.  0.
28    NH3       0.000d+00 0.000d+00 -1.000d+00 1.000d+00  0.000d+00  0.000d+00  0.000d+00  0.000d+00  3.  0.
29    N2O5      0.000d+00 0.000d+00 -1.000d+00 1.000d+00  0.000d+00  0.000d+00  0.000d+00  0.000d+00  0.  5.
30    NH4NO2    0.000d+00 0.000d+00 -1.000d+00 1.000d+00  0.000d+00  0.000d+00  0.000d+00  0.000d+00  4.  2.
31    NH4NO3    0.000d+00 0.000d+00 -1.000d+00 1.000d+00  0.000d+00  0.000d+00  0.000d+00  0.000d+00  4.  3.
32    NO2-      0.000d+00 0.000d+00 -1.000d+00 1.000d+00  0.000d+00  0.000d+00  0.000d+00  0.000d+00  0.  2.
33    N2+       0.000d+00 0.000d+00 -1.000d+00 1.000d+00  0.000d+00  2.270d+00  0.000d+00  0.000d+00  0.  0.
34    NO+       0.000d+00 0.000d+00 -1.000d+00 1.000d+00  0.000d+00  0.000d+00  0.000d+00  0.000d+00  0.  1.
35    N+        0.000d+00 0.000d+00 -1.000d+00 1.000d+00  0.000d+00  0.690d+00  0.000d+00  0.000d+00  0.  0.
36    CO2       8.172d-08 8.172d-08 -1.000d+00 1.000d+00  0.000d+00  0.000d+00  0.000d+00 -7.470d+00  0.  2.
37    CO        0.000d+00 0.000d+00 -1.000d+00 1.000d+00  0.000d+00  0.000d+00  0.000d+00  4.720d+00  0.  1.
38    CO+       0.000d+00 0.000d+00 -1.000d+00 1.000d+00  0.000d+00  0.000d+00  0.000d+00  0.510d+00  0.  1.
39    CO2+      0.000d+00 0.000d+00 -1.000d+00 1.000d+00  0.000d+00  0.000d+00  0.000d+00  2.240d+00  0.  2.
40    He        2.043d-01 2.043d-01 -1.000d+00 1.000d+00  0.000d+00  0.000d+00  0.000d+00  0.000d+00  0.  0.
```